Electronic Supplementary Information

A Schiff base platform: structures, sensing of Zn(II), PPi in aqueous medium and anticancer activity

Barnali Naskar[a], Ritwik Modak[a], Dilip K. Maiti[a], Michael G. B. Drew[b], Antonio Bauzá[c], Antonio Frontera[c], Chitrangada Das Mukhopadhyay[d], Snehasis Mishra[e], Krishna Das Saha[e], and Sanchita Goswami[*,a]

[a]Department of Chemistry, University of Calcutta, 92, A. P. C. Road, Kolkata – 700009, India

[b]Department of Chemistry, University of Reading, Whiteknights, Reading RG6 6AD, U.K.

[c]Departament de Química, Universitat de les IllesBalears, Crta. deValldemossa km 7.5, 07122 Palma de Mallorca, Baleares, Spain

[d]Centre for Healthcare Science & Technology, Indian Institute of Engineering Science and Technology, Shibpur Howrah 711103, India

[e]Cancer and Inflammatory Disorder Division, CSIR-Indian Institute of Chemical Biology, Jadavpur, Kolkata 700032, West Bengal, India. E-mail: krishna@iicb.res.in

Contents of the Supporting Information

1. Characterization, Structure and Crystallographic Data

Pages

2. PhotophysicalCharacterization

3. Cell Study

1.Characterization, Structure and Crystallographic Data.

^{1}H and ^{13}C−NMR spectra: H_2Vd were dissolved in d_6–DMSO and recorded with TMS as internal standard on a Bruker, AV 300 Supercon Digital NMR system.

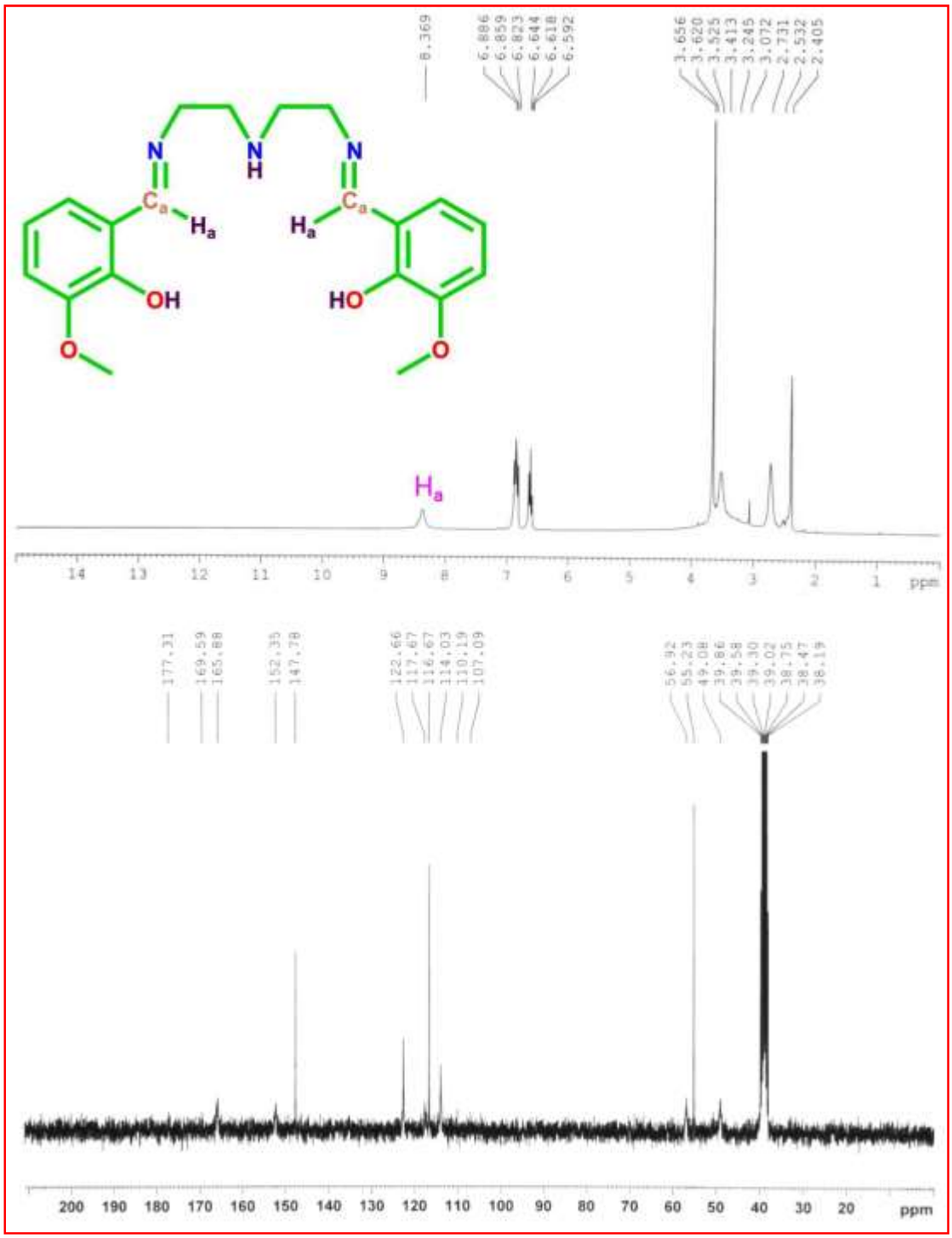

Figure S1. ^{1}H and ^{13}C−NMR spectrum of chemosensor **H_2Vd**.

1.Characterization, Structure and Crystallographic Data.

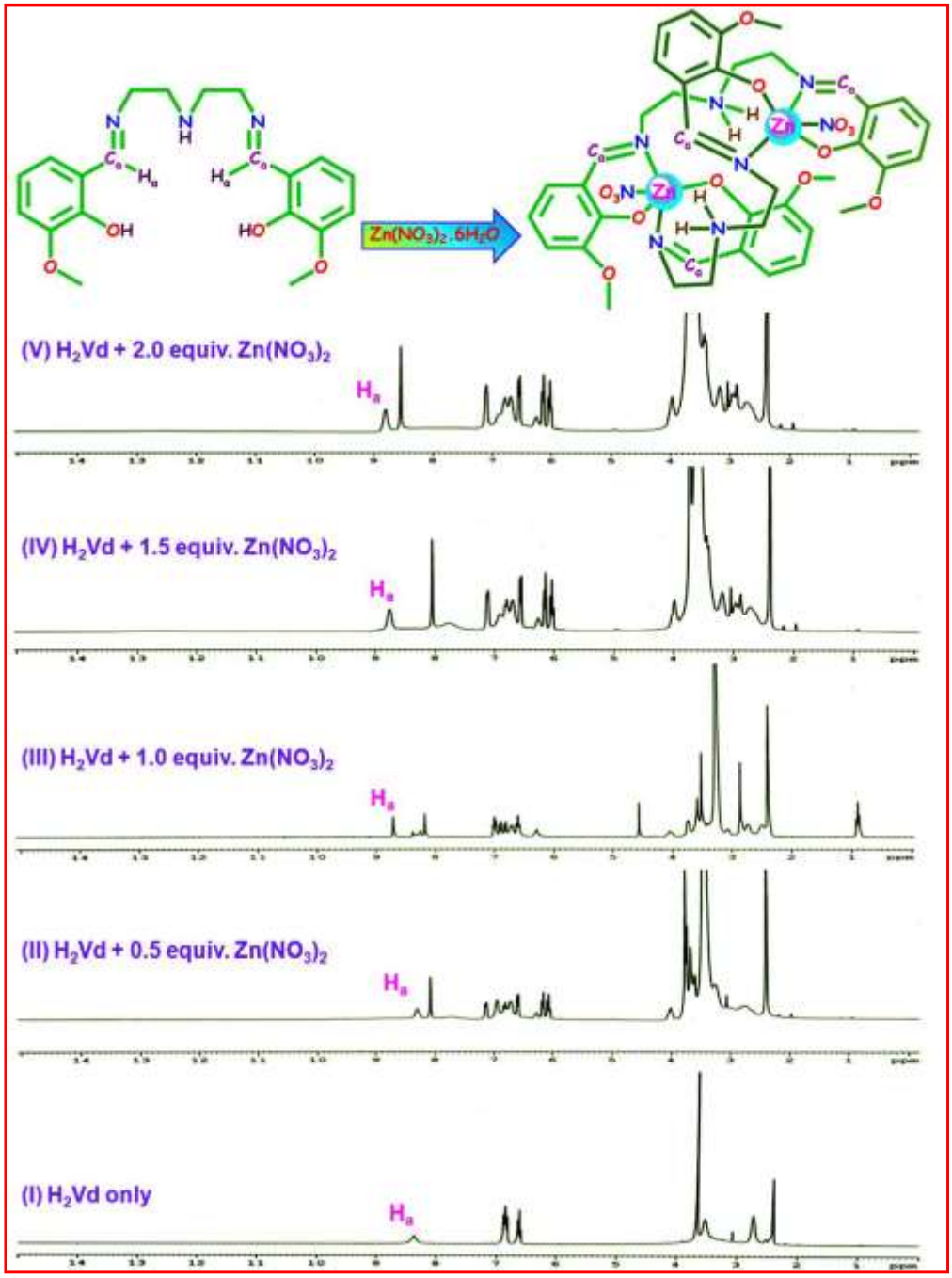

Figure S2. ^{1}H−NMR titration of **H_2Vd** with $Zn(NO_3)_2.6H_2O$ in DMSO−d_6 solution.

1.Characterization, Structure and Crystallographic Data.

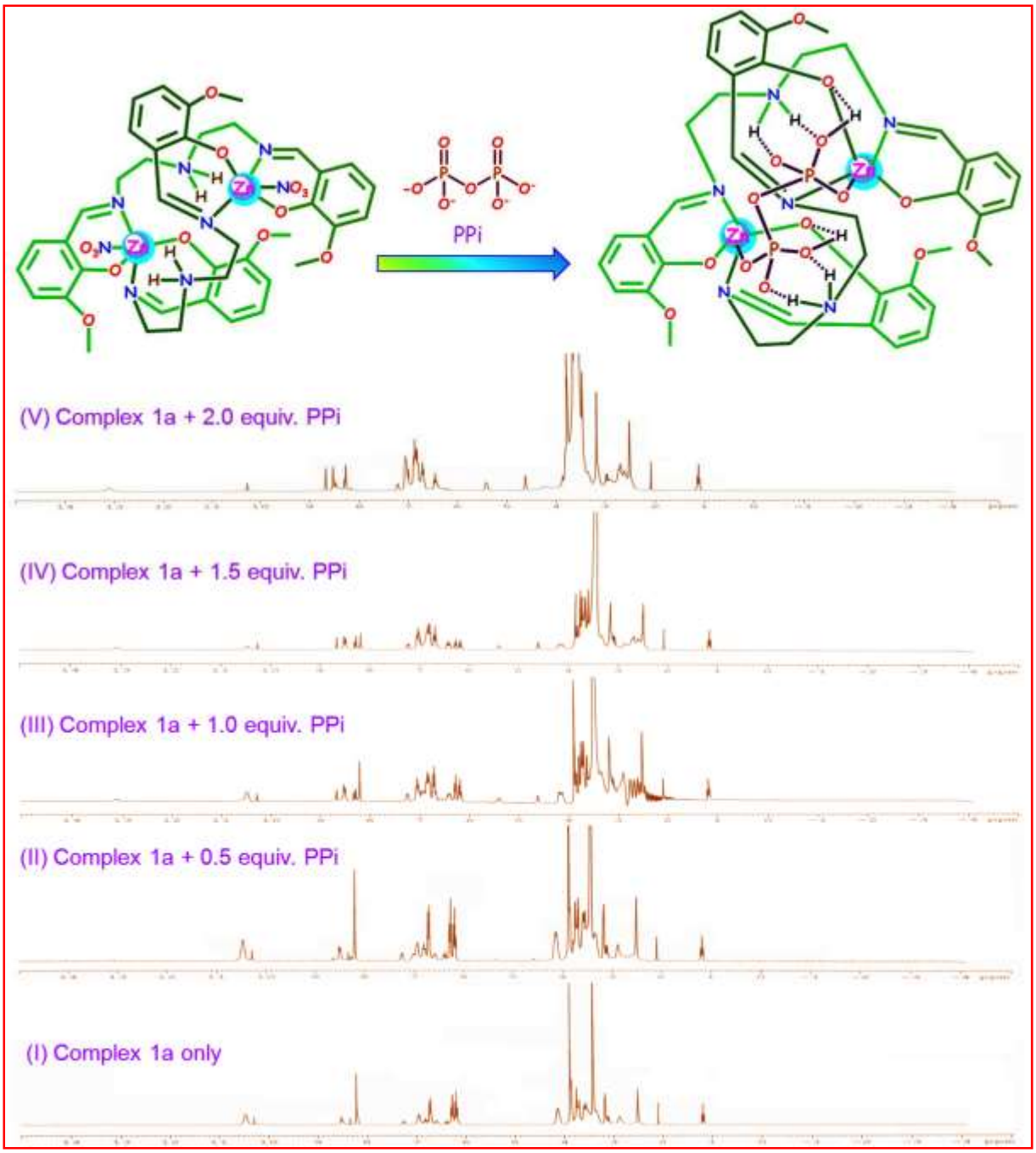

Figure S3. ^{1}H−NMR titration of complex **1a** with PPi in DMSO−d_6 solution.

1.Characterization, Structure and Crystallographic Data.

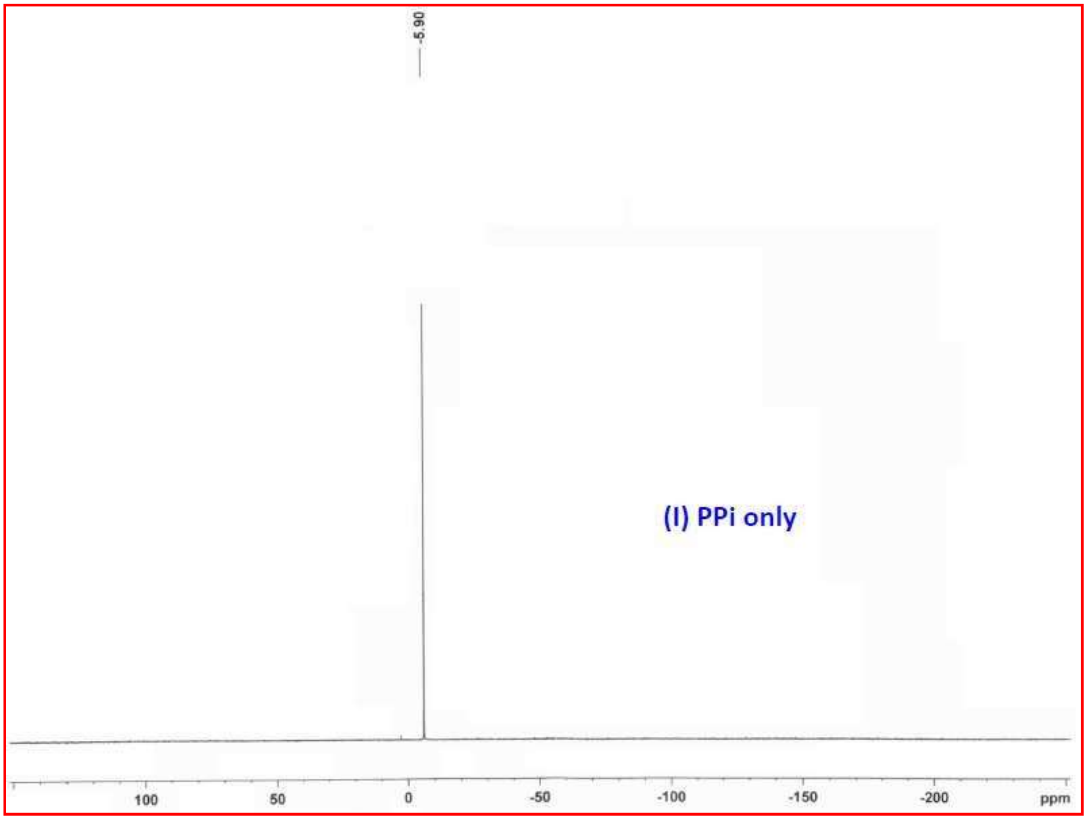

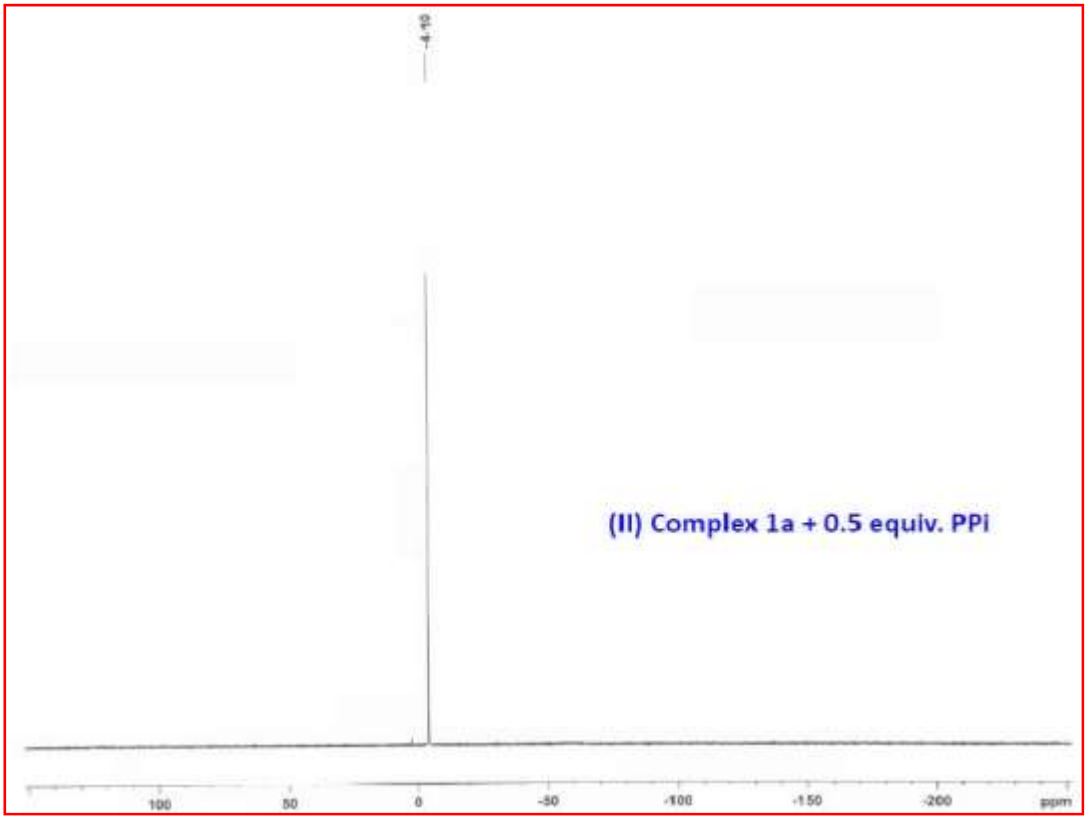

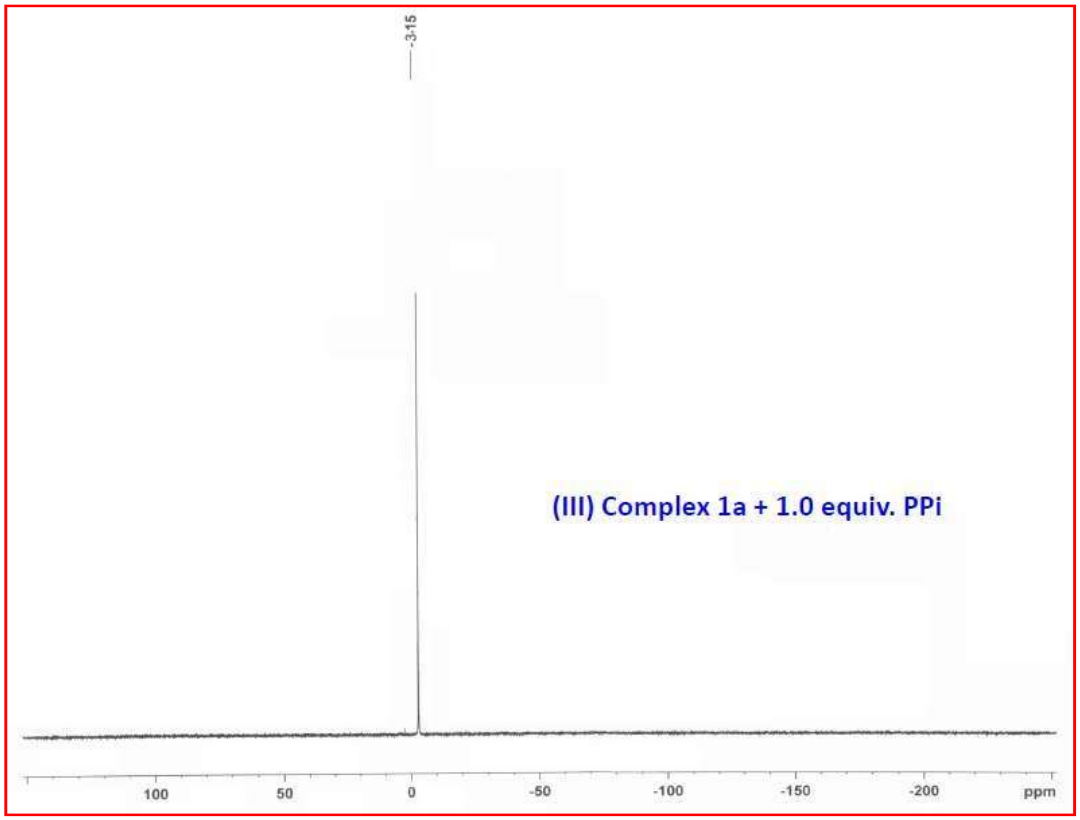

Figure S4. ^{31}P−NMR titration of complex **1a** with PPi in D_2O solution.

1. Characterization, Structure and Crystallographic Data.

FT−IR spectroscopy: Fourier transform infrared (FT−IR) spectra were recorded with a Perkin−Elmer RXI FT−IR spectrophotometer using the reflectance technique (4000−400 cm^{-1}). Samples were prepared as KBr disks.

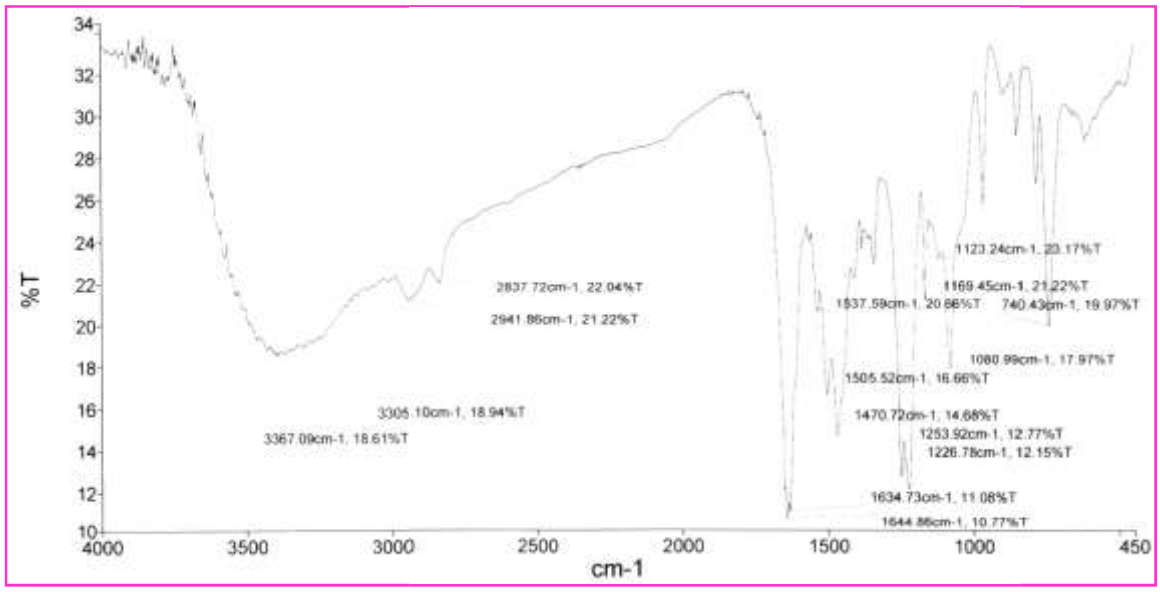

H_2Vd

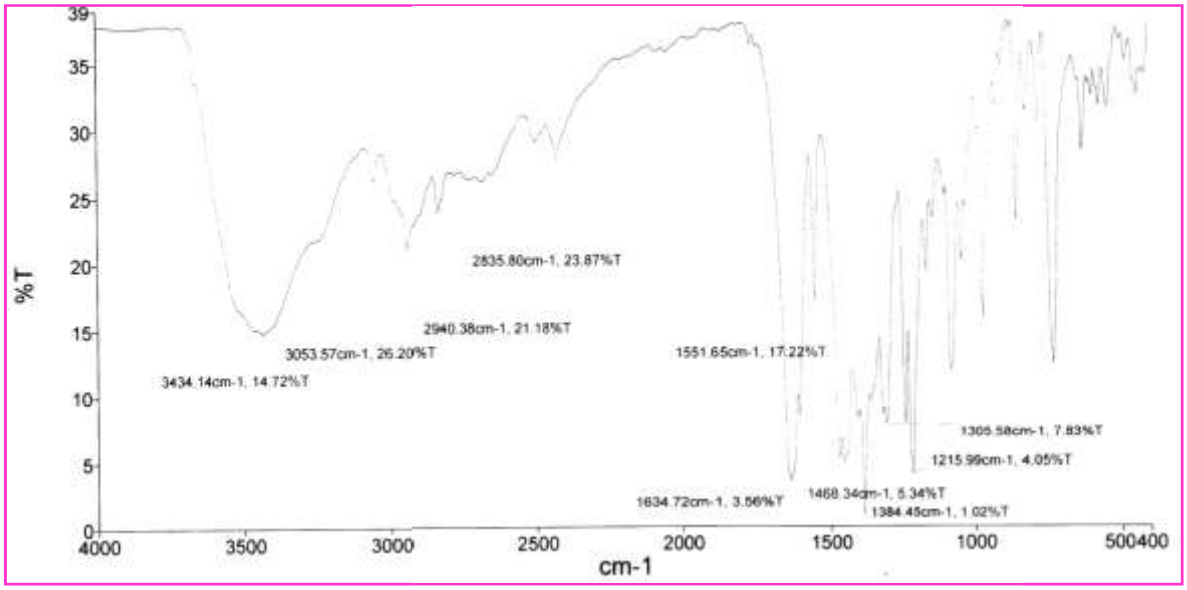

(1a)

1. Characterization, Structure and Crystallographic Data.

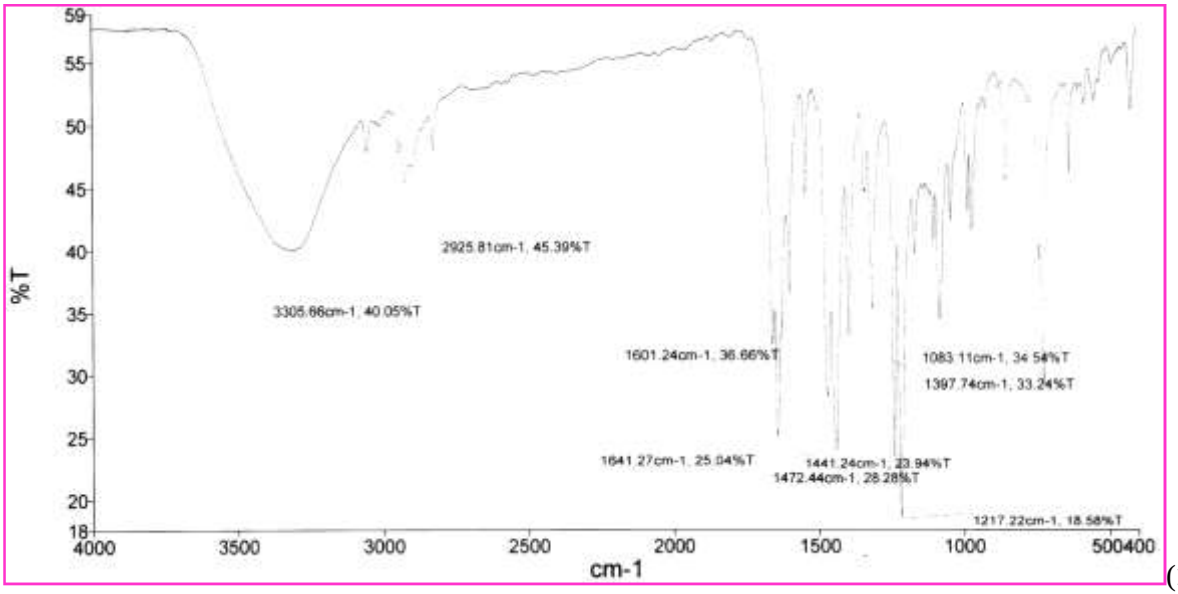

(1b)

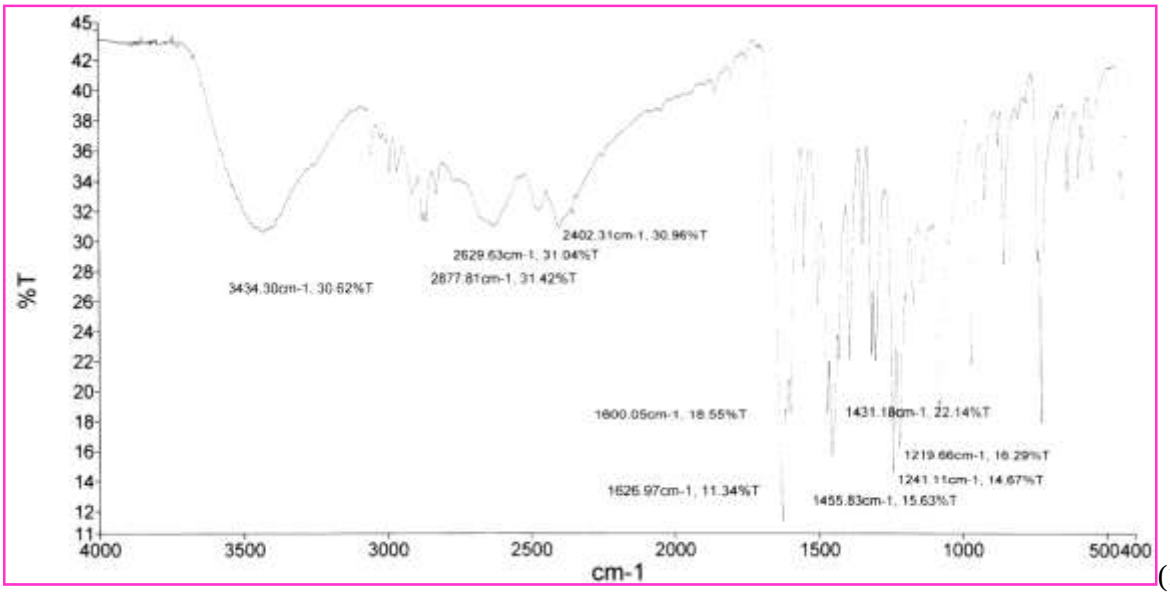

(1c)

1. Characterization, Structure and Crystallographic Data.

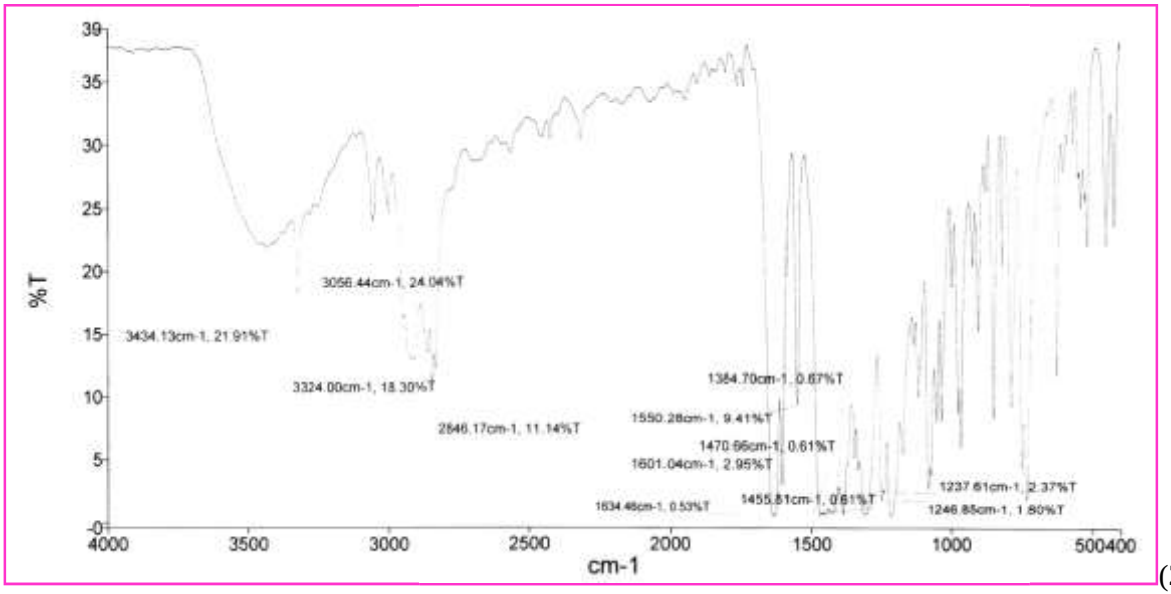

(2)

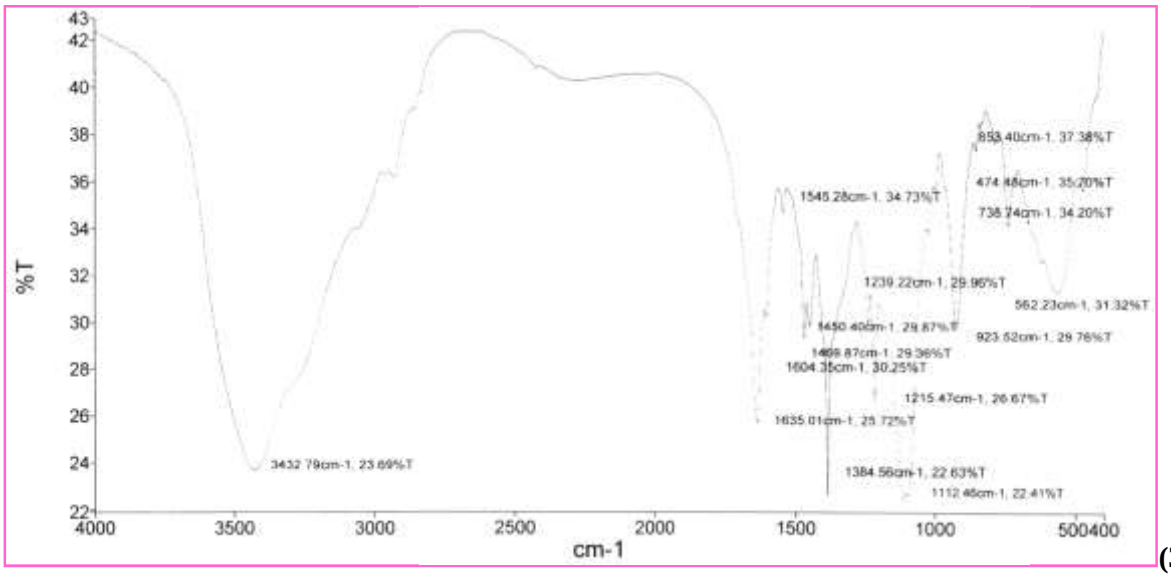

(3)

Figure S5. FT−IR Spectrum of **H_2Vd**, complexes **1(a-c)**, **2** and **PPi complex (3)**.

1. Characterization, Structure and Crystallographic Data.

Electrospray ionization mass spectra: (HR–ESI–MS) were recorded on Qtof Micro YA263 mass spectrometer dissolving the samples in LC–MS quality water.

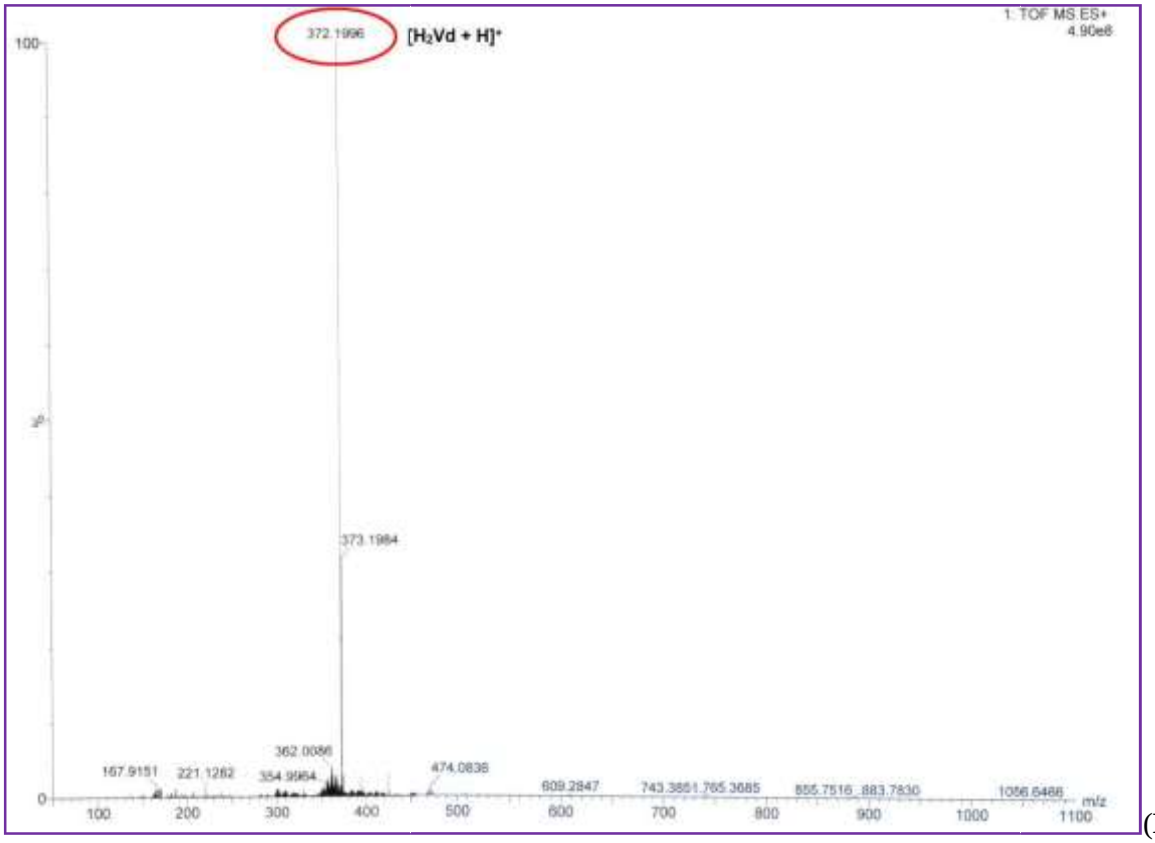

(**H_2Vd**)

1. Characterization, Structure and Crystallographic Data.

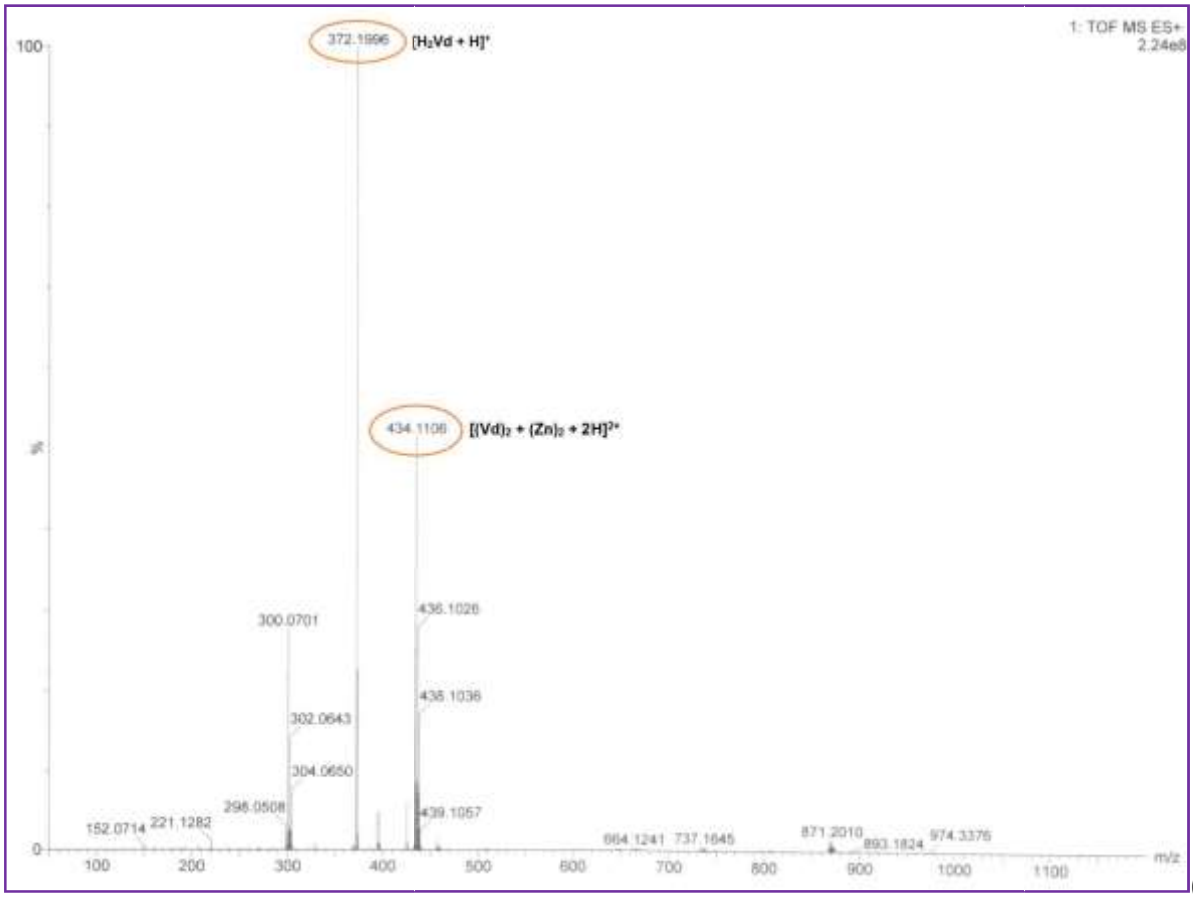

(**1a**)

1. Characterization, Structure and Crystallographic Data.

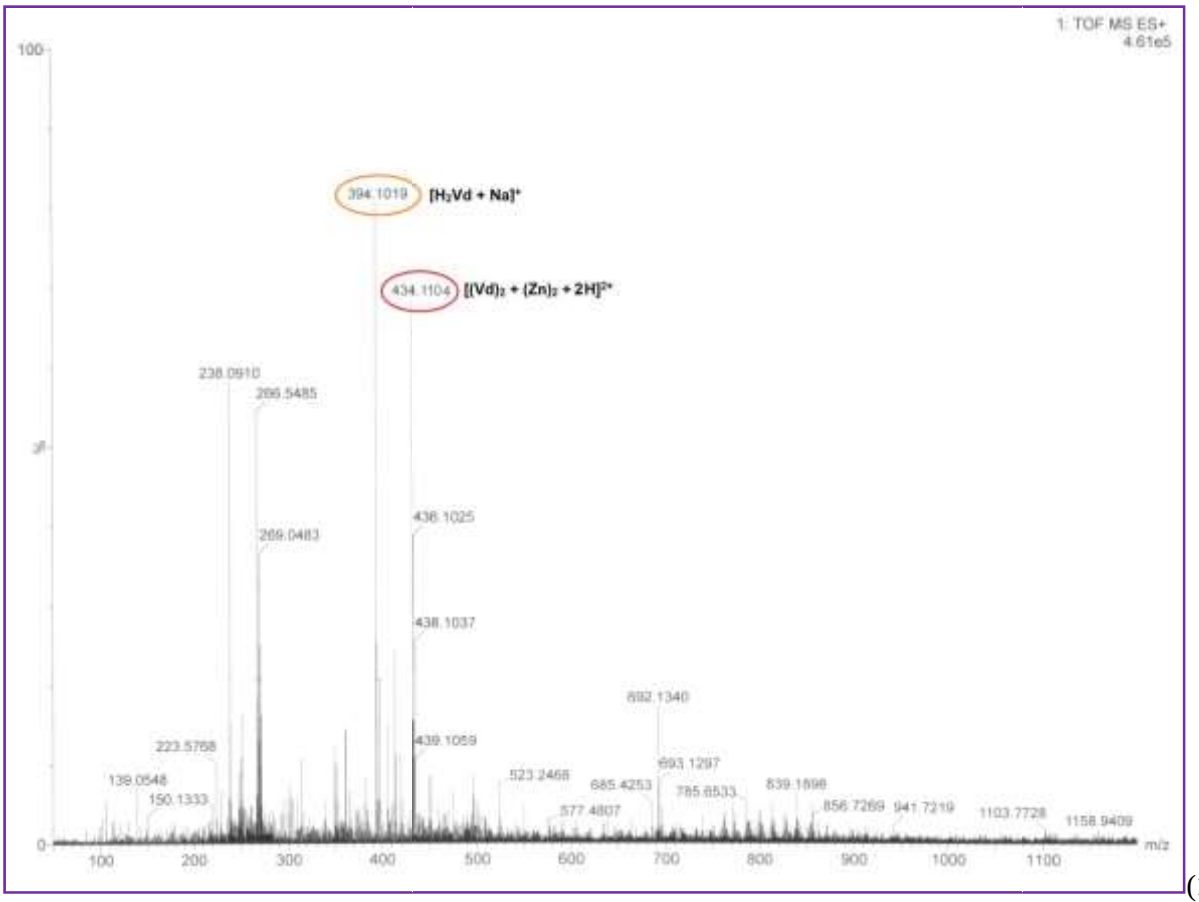

(**1b**)

1. Characterization, Structure and Crystallographic Data.

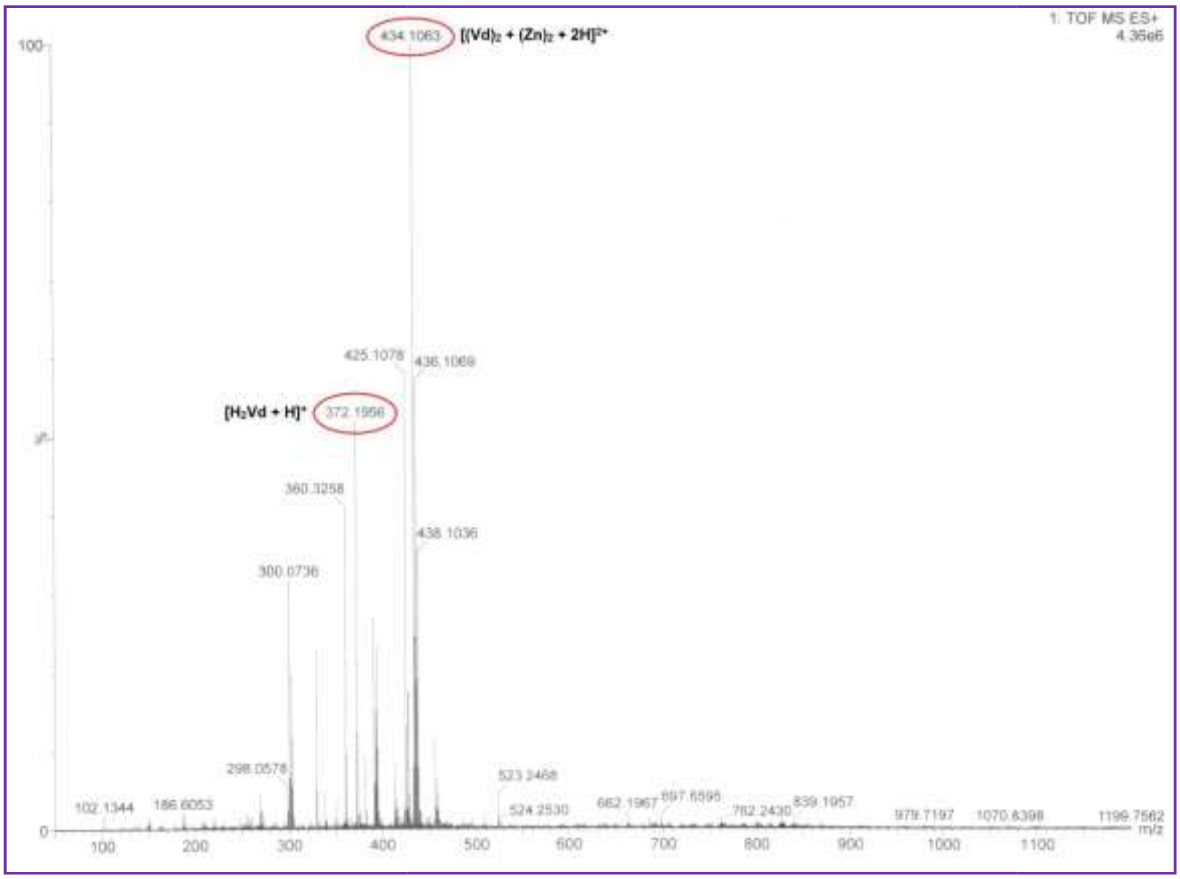

(**1c**)

1. Characterization, Structure and Crystallographic Data.

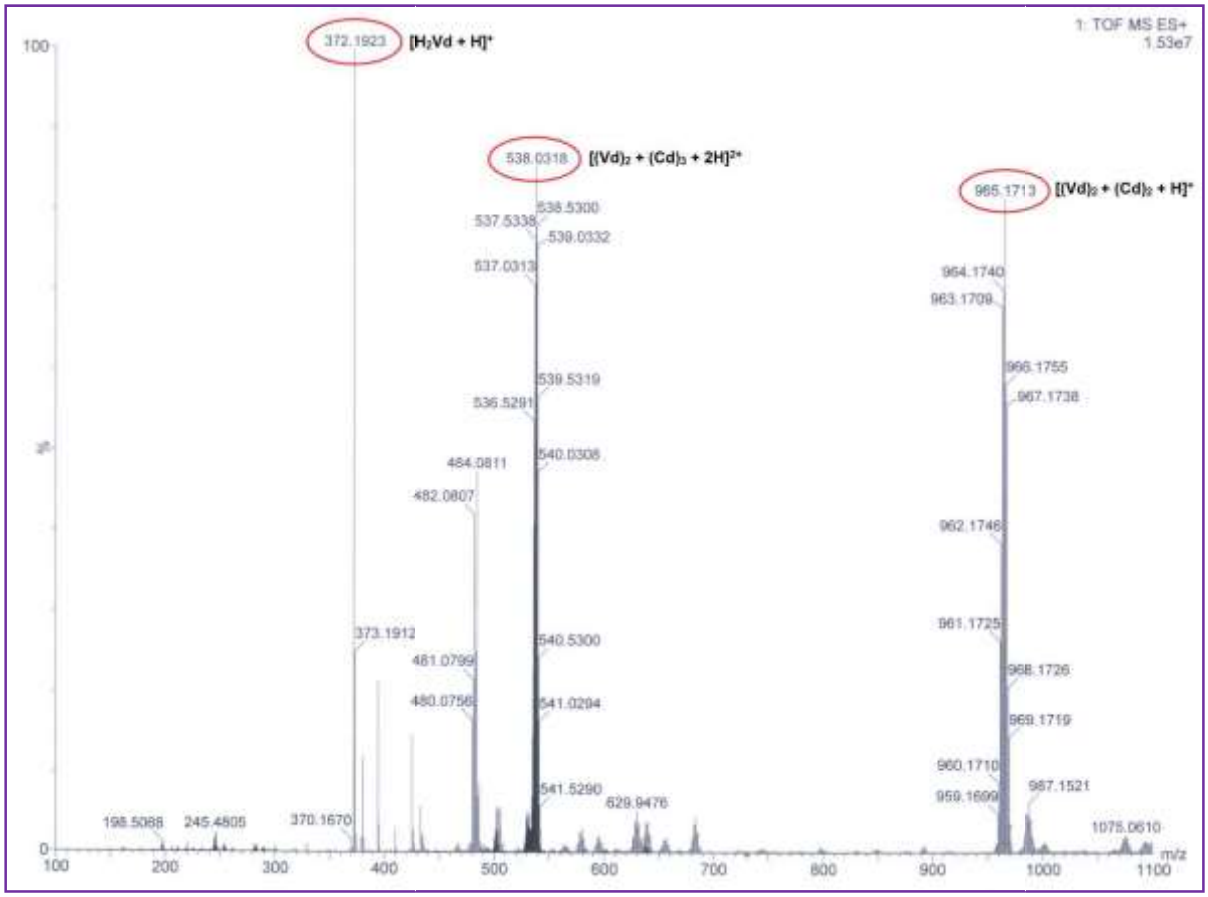

(**2**)

1. Characterization, Structure and Crystallographic Data.

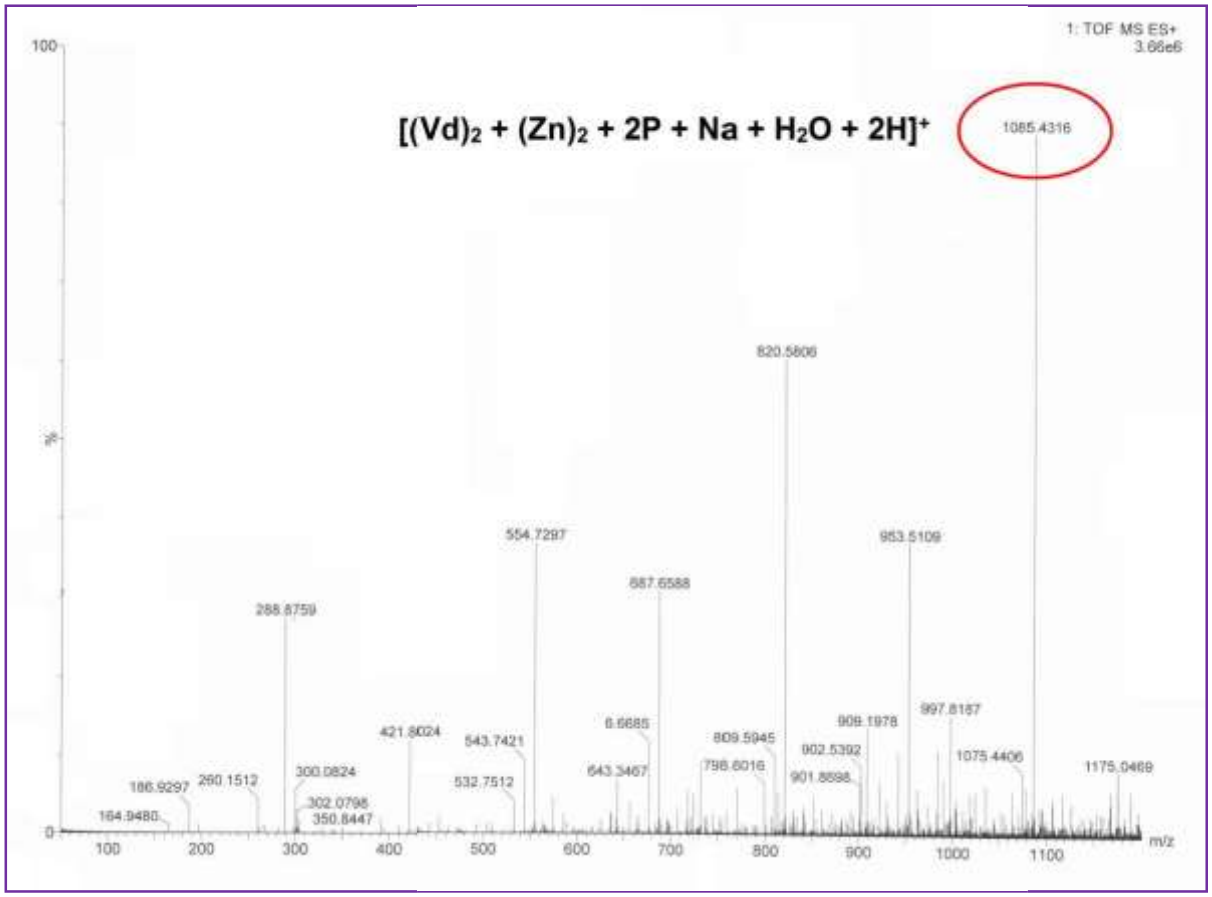

(3)

Figure S6. ESI–MS of ligand (**H_2Vd**) in complexes **1(a-c)**, **2** and **PPi complex (3)**.

1. Characterization, Structure and Crystallographic Data.

Powder X−ray diffraction: (PXRD) patterns were recorded on a PANalytical, XPERT–PRO diffractometer with Cu K_α radiation (40 kV, 30 mA, λ = 1.5406 Å).

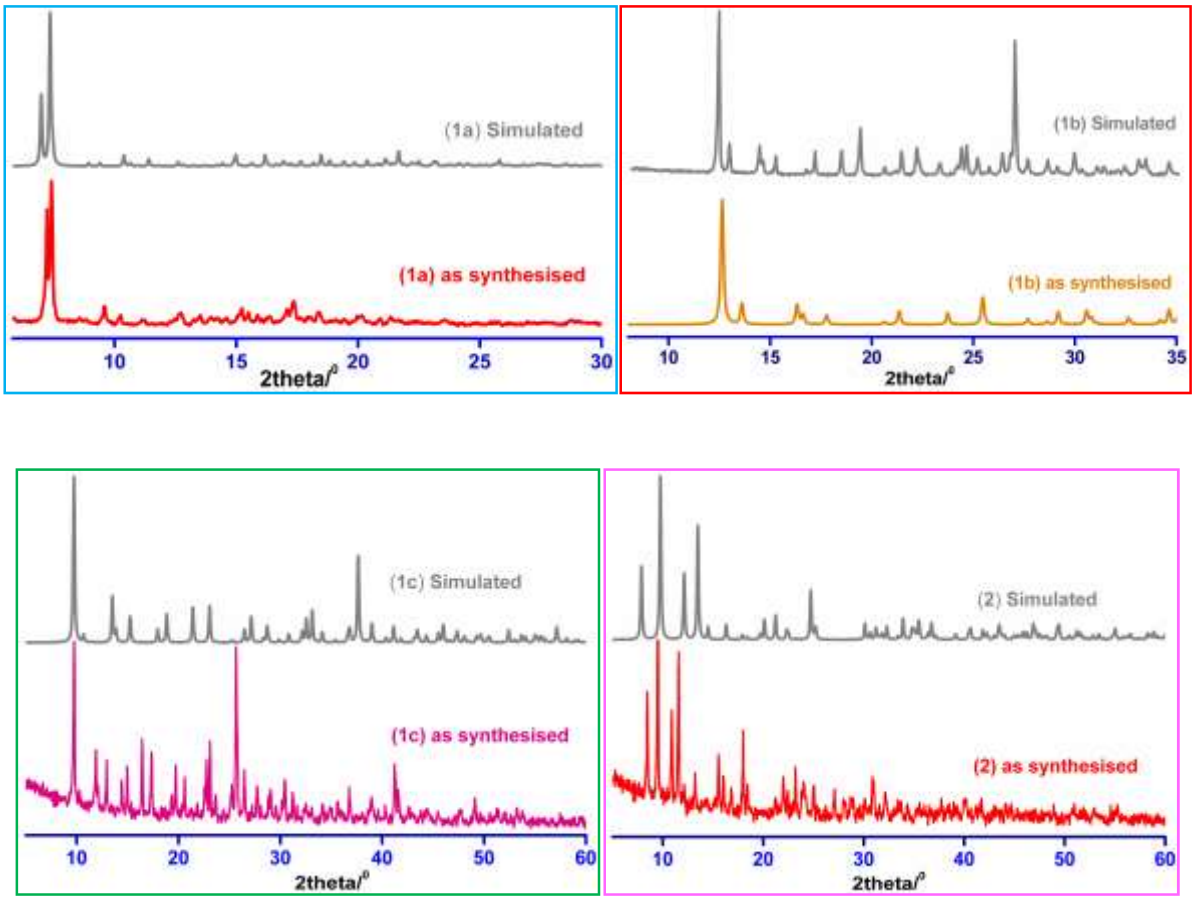

Figure S7. PXRD pattern of complexes **1(a-c)** and **2** vs. simulated pattern.

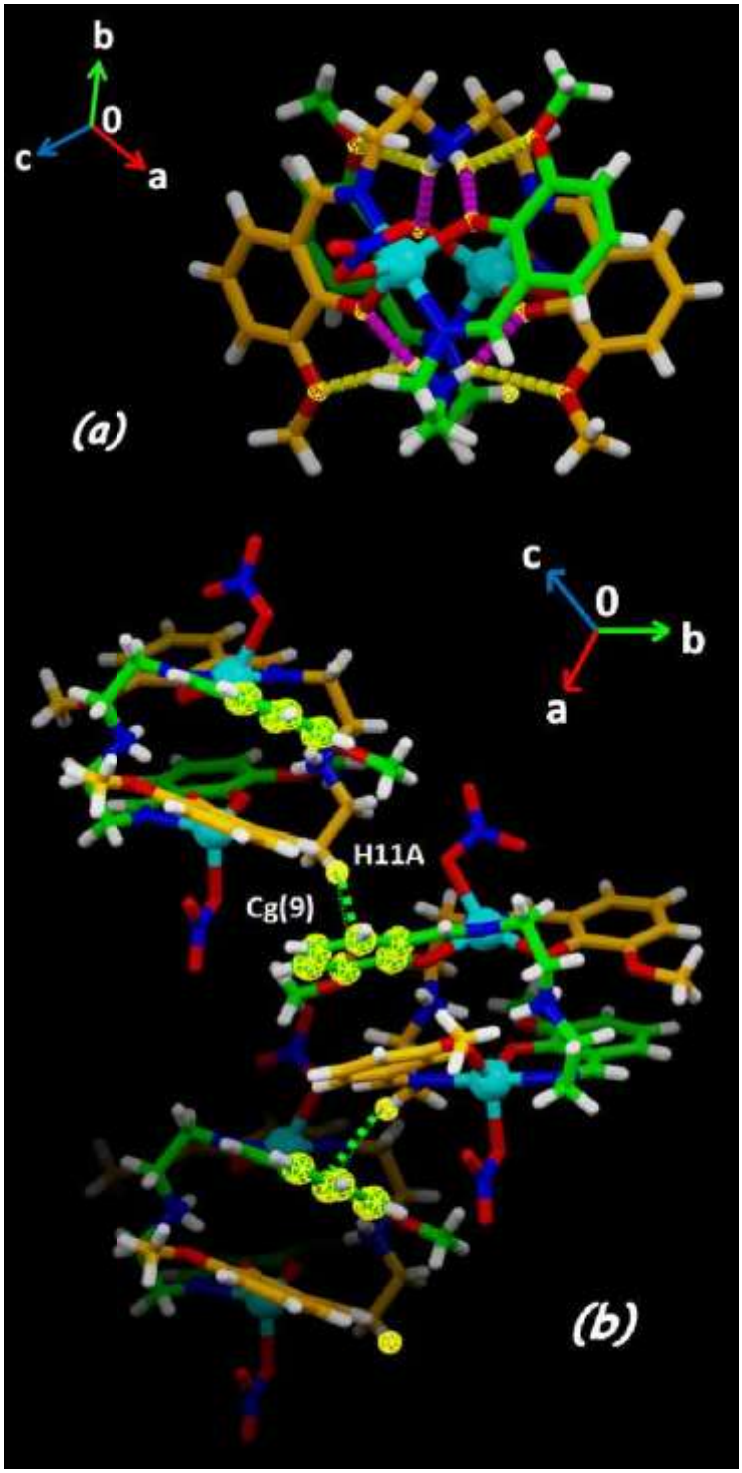

Figure S8. Packing in complex **1a** (**a**) Intra-molecular hydrogen bonds (where dotted pink lines and dotted yellow lines respectively represent strong and comparatively weak hydrogen bonds). (**b**) Formation of 1D Chain through intra-molecular C–H···π interactions (shown as dotted green lines).

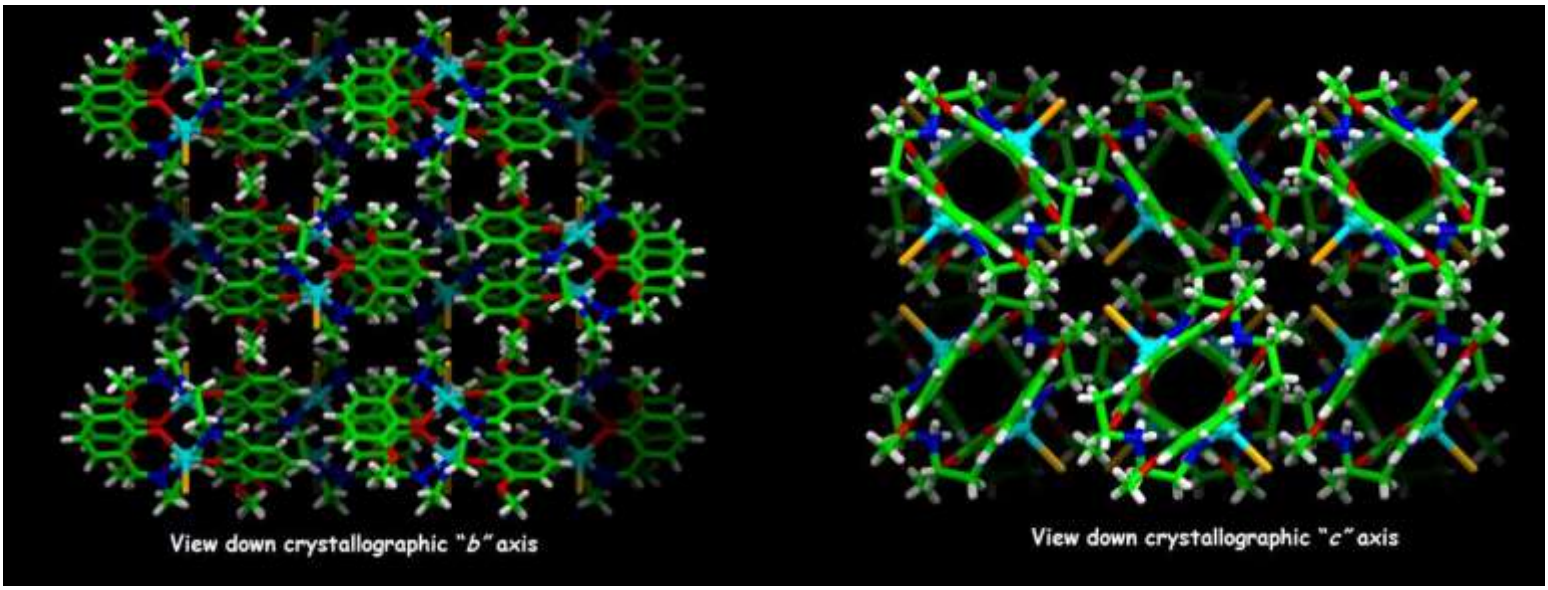

Figure S9. Molecular representation of crystal packing down crystallographic 'b' and 'c' axes in complex **1c** (complex **1b** is isostructural).

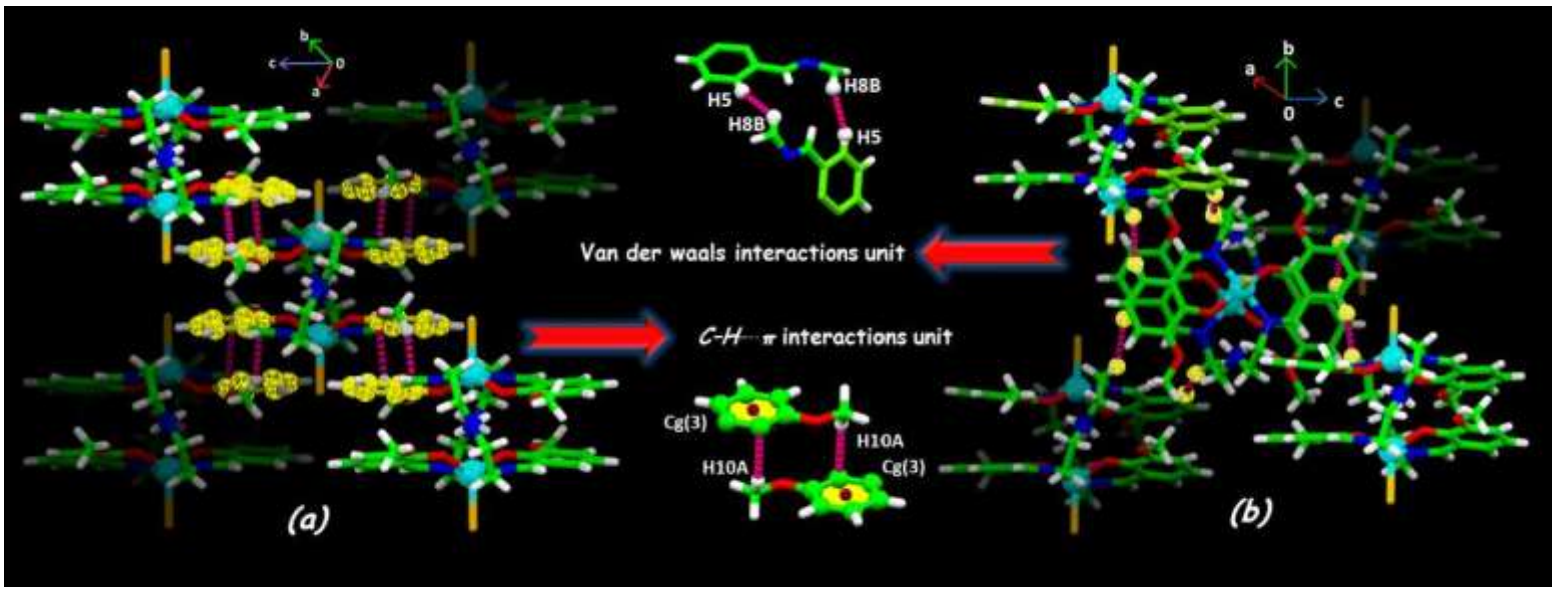

Figure S10. The inter-molecular (a) C – H···π and (b) Van der Waals interactions in complex **1b**.

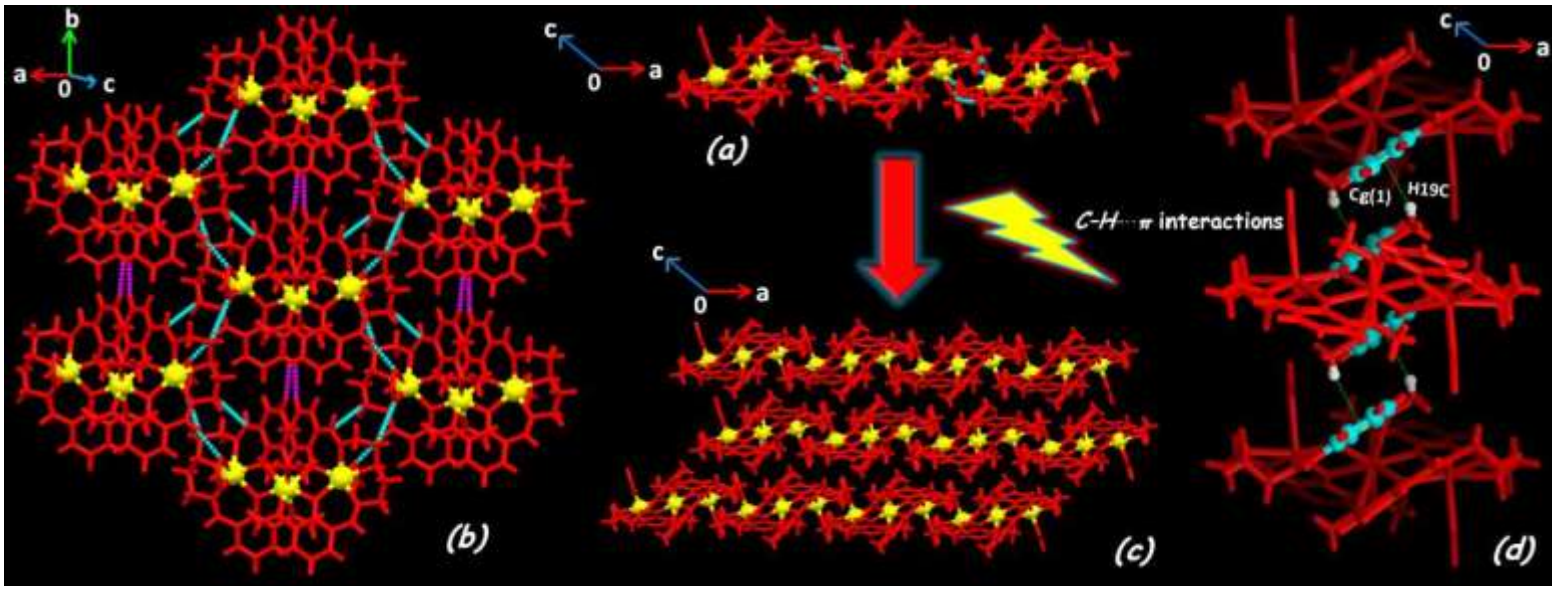

Figure S11. (**a**) 2D Sheet view along crystallographic b axis of complex **2**. (**b**) The H-bonds (light blue) and van der Waals (pink) interactions within 2D sheet of complex **2**. (**c**) 3D packing constituted by 2D sheets connected via intermolecular C – H···π interactions. (**d**) The C – H···π interactions between the 2D Sheets.

Table S1. ^{1}H and ^{13}C−NMR shift data of NMR titration experiment of **H_2Vd**.

^{1}H						
Proton label	**Free H_2Vd (ppm) (A)**	**H_2Vd + 0.5 equiv. $Zn(NO_3)_3 \cdot 6H_2O$ (ppm) (B)**	**H_2Vd + 1.0 equiv. $Zn(NO_3)_3 \cdot 6H_2O$ (ppm) (C)**	**H_2Vd + 1.5 equiv. $Zn(NO_3)_3 \cdot 6H_2O$ (ppm) (D)**	**H_2Vd + 2.0 equiv. $Zn(NO_3)_3 \cdot 6H_2O$ (ppm) (E)**	**Shift (E−A) (ppm)**
H_a	8.369	8.454	8.714	8.717	8.719	0.35 **downfield**
^{13}C						
C_a	177.31	178.90	192.21	195.54	202.01	24.7 **downfield**

1. Characterization, Structure and Crystallographic Data.

Table S2. Single Crystal X–ray diffraction: Crystallographic data for complexes **1(a-c)** and **2**.

	Complex (1a)	**Complex (1b)**	**Complex (1c)**	**Complex (2)**
Chemical formula	$C_{40.5}H_{50}N_8O_{14.5}Zn_2$	$C_{40}H_{48}Br_2N_6O_8Zn_2$	$C_{40}H_{48}I_2N_6O_8Zn_2$	$C_{40}H_{46}Cd_3N_8O_{14}$
CCDC	1541737	1541738	1541742	1541744
Formula weight	1011.62	1031.42	1125.38	1200.05
Temperature/K	150(2)	150(2)	150(2)	150(2)
λ^a/ Å	0.71073	0.71073	0.71073	0.71073
Crystal system	monoclinic	tetragonal	tetragonal	monoclinic
Space group	$P2_1/c$	$I4_1/acd$	$I4_1/acd$	C2/c
***a* (Å)**	11.2108(8)	17.3167(7)	17.5829(8)	22.4096(8)
***b*(Å)**	28.827(2)	17.3167(7)	17.5829(8)	12.5242(4)
***c*(Å)**	14.9281(16)	27.7850(18)	27.888(3)	16.1728(7)
β (°)	109.109(10)	90.00	90.00	106.738(4)
Z	4	8	8	4
***V* (Å^3)**	4558.5(7)	8331.8(7)	8621.8(10)	4346.8(3)
ρ calc(g/cm^3)	1.474	1.644	1.734	1.834
μ(mm^{-1})	1.127	3.129	2.602	1.531
***F*(000)**	2100	4192	4480	2392
θ min−max (°)	3.46 to 30.00	3.76 to 30.00	3.73 to 30.00	3.45 to 30.00
Reflns collected	30046	8220	9763	14694
Independent reflns	12895	2900	3117	6284
R(int)	0.0836	0.0638	0.0548	0.0252
S(GOF)	1.002	1.143	1.071	1.076
***R1, wR2*(I>2σ(I))^b**	0.0736^b, 0.1486^c	0.0665^b, 0.0973^c	0.0514 ^{b}, 0.0905^c	0.0454 ^{b}, 0.0953^c
***R1, wR2*(all data)^b**	0.1380^b, 0.1726^c	0.1138^b, 0.1079^c	0.0896 ^{b}, 0.1008^c	0.0547 ^{b}, 0.0993^c
largest diff peak, hole/e Å^{-3}	0.852 and -0.707	0.444 and -0.673	0.482 and -0.827	3.460 and -1.885

^{a}Graphite monochromator, $^bR_1 = \Sigma(|F_o| - |F_c|)/\Sigma|F_o|$. $^cwR_2 = \{\Sigma[w(|F_o|^2 - |F_c|^2)^2]/\Sigma[w(|F_o|^2)^2]\}^{1/2}$

Table S3. Bond distances (Å) and angles (^{0}) in the metal coordination spheres of complexes **1(a-c)** and **2**.

Complex (1a)		Complex (1b)		Complex (1c)		Complex (2)	
Zn(1)–O(1)	1.995(3)	Zn(1)–O(1)	1.992(2)	Zn(1)–O(1)	1.986(3)	Cd(1)–O(1)	2.203(2)
Zn(1)–O(5)	1.986(3)	Zn(1)–N(1)	2.135(3)	Zn(1)–N(1)	2.135(3)	Cd(1)–O(2)	2.287(2)
Zn(1)–O(9)	2.267(3)	Zn(1)–Br(2)	2.4595(8)	Zn(1)–I(2)	2.6710(7)	Cd(1)–O(3)	2.740(3)
Zn(1)–N(1)	2.071(4)	Br(2)–Zn(1)–O(1)	115.14(7)	I(2)–Zn(1)–O(1)	115.09(7)	Cd(1)–O(4)	2.451(3)
Zn(1)–N(4)	2.072(4)	Br(2)–Zn(1)–N(1)	95.83(8)	I(2)–Zn(1)–N(1)	95.03(8)	Cd(2)–O(1)	2.236(2)
Zn(2)–O(2)	2.009(3)	O(1)–Zn(1)–N(1)	86.64(11)	O(1)–Zn(1)–N(1)	86.35(12)	Cd(2)–O(2)	2.350(2)
Zn(2)–O(6)	2.001(3)	O(1)-Zn(1)-O(1)[a]	129.72(15)	O(1)-Zn(1)-O(1)[a]	129.82(15)	Cd(2)–O(5C)	2.347(3)
Zn(2)–O(12)	2.196(3)	O(1)-Zn(1)-N(1)[a]	88.38(10)	O(1)-Zn(1)-N(1)[a]	89.39(12)	Cd(2)–O(6C)	2.751(4)
Zn(2)–N(3)	2.081(3)	N(1)-Zn(1)-N(1)[a]	168.34(16)	N(1)-Zn(1)-N(1)[a]	169.94(16)	Cd(2)–N(1)	2.299(3)
Zn(2)–N(6)	2.074(3)	[a]symmetry element 1-x, 1/2-y, z		[a]symmetry element 1-x, 1/2-y,z		Cd(2)– N(2)	2.523(4)
O(5)–Zn(1)–O(1)	128.27(11)					Cd(2)– N(3)	2.313(4)
O(5)–Zn(1)–N(1)	93.16(13)					O(1)–Cd(1)–O(2)	72.56(9)
O(1)–Zn(1)–N(1)	88.42(13)					O(1)–Cd(1)–O(3)	61.45(9)
O(5)–Zn(1)–N(4)	89.79(13)					O(1)–Cd(1)–O(4)	138.74(9)
O(1)–Zn(1)–N(4)	91.90(13)					O(2)–Cd(1)–O(3)	125.24(9)
N(1)–Zn(1)–N(4)	175.98(13)					O(2)–Cd(1)–O(4)	67.04(9)
O(5)–Zn(1)–O(9)	90.51(12)					O(3)–Cd(1)–O(4)	155.18(10)
O(1)–Zn(1)–O(9)	141.18(12)					O(1)-Cd(1)-O(1)[a]	99.27(14)
N(1)–Zn(1)–O(9)	87.61(13)					O(1)-Cd(1)-O(2)[a]	137.18(9)
N(4)–Zn(1)–O(9)	89.63(13)					O(2)-Cd(1)-O(2)[a]	140.87(12)
O(6)–Zn(2)–O(2)	128.39(12)					O(1)-Cd(1)-O(4)[a]	104.47(10)
O(6)–Zn(2)–N(6)	90.07(12)					O(2)-Cd(1)-O(4)[a]	82.66(10)
O(2)–Zn(2)–N(6)	89.31(13)					O(4)-Cd(1)-O(4)[a]	78.70(15)
O(6)–Zn(2)–N(3)	90.44(12)					O(1)-Cd(1)-O(3)[a]	80.71(9)
O(2)–Zn(2)–N(3)	88.16(13)					O(2)-Cd(1)-O(3)[a]	75.74(9)
N(6)–Zn(2)–N(3)	177.14(14)					O(4)-Cd(1)-O(3)[a]	81.70(9)
O(6)–Zn(2)–O(12)	97.53(12)					O(3)-Cd(1)-O(3)[a]	120.85(12)
O(2)–Zn(2)–O(12)	134.07(11)					O(1)–Cd(2)–O(2)	70.78(9)
N(6)–Zn(2)–O(12)	92.14(12)					O(1)–Cd(2)–O(5C)	94.31(12)
N(3)–Zn(2)–O(12)	90.58(12)					O(1)–Cd(2)–O(6C)	79.93(11)
						O(1)–Cd(2)–N(1)	77.57(11)
						O(1)–Cd(2)–N(2)	141.69(11)
						O(1)–Cd(2)–N(3)	146.25(10)
						O(2)–Cd(2)–O(5C)	97.70(11)
						O(2)–Cd(2)–O(6C)	133.18(11)
						O(2)–Cd(2)–N(1)	119.90(10)
						O(2)–Cd(2)–N(2)	145.15(11)
						O(2)–Cd(2)–N(3)	76.92(10)
						O(5C)–Cd(2)–O(6C)	48.27(11)
						O(5C)–Cd(2)–N(1)	135.01(12)
						O(5C)–Cd(2)–N(2)	92.45(13)
						O(5C)–Cd(2)–N(3)	80.38(12)
						O(6C)–Cd(2)–N(1)	86.83(12)
						O(6C)–Cd(2)–N(2)	76.80(12)

						O(6C)–Cd(2)–N(3)	117.52(11)
						N(1)–Cd(2)–N(2)	71.18(12)
						N(1)–Cd(2)–N(3)	128.83(12)
						N(2)–Cd(2)–N(3)	72.05(12)
						Cd(1)–O(1)–Cd(2)	111.75(11)
						Cd(1)–O(2)–Cd(2)	104.83(10)
						[a]symmetry element 1-x, y, 1/2-z	

Table S4. Results of Continuous Shape Measurement analysis for the Zn(II) and Cd(II) coordination spheres in complexes **1(a-c)** and **2**.

Shape analysis : Continuous Shape Measurement (CShM)[a] of coordination sphere using SHAPE v2.1.

For Zn1 and Zn2 in complex **1a**

```
-------------------------------------------------------------------------------
S H A P E   v2.1         Continuous Shape Measures calculation
(c) 2013 Electronic Structure Group, Universitat de Barcelona
                   Contact:  llunell@ub.edu
-------------------------------------------------------------------------------

Zn2L2(NO3) structures

PP-5        1    D5h      Pentagon
vOC-5       2    C4v      Vacant octahedron
TBPY-5      3    D3h      Trigonal bipyramid
SPY-5       4    C4v      Spherical square pyramid
JTBPY-5     5    D3h      Johnson trigonal bipyramid J12

For Zn1
Structure [ML5]         PP-5         vOC-5       TBPY-5        SPY-5      JTBPY-5
Complex (1a),           29.952,        4.825,      1.385,         4.091,      3.999

For Zn2
Structure [ML5]        PP-5          vOC-5       TBPY-5        SPY-5      JTBPY-5
Complex (1a),          28.032,         3.433,      2.413,         3.089,      4.983


Zn2L3(NO3) structures

HP-6            1 D6h   Hexagon
PPY-6           2 C5v   Pentagonal pyramid
OC-6            3 Oh    Octahedron
TPR-6           4 D3h   Trigonal prism
JPPY-6          5 C5v   Johnson pentagonal pyramid J2

For Zn1
Structure [ML6]        HP-6        PPY-6         OC-6        TPR-6       JPPY-6
Complex (1a),          34.695,      20.027,        5.312,       9.020,      23.654

For Zn2
Structure [ML6]        HP-6        PPY-6         OC-6        TPR-6       JPPY-6
Complex (1a),          34.517,     21.444,         4.776,       9.274,      25.089
```

[a]CShM values between 0.1 and 3 usually correspond to a not negligible but still small distortion from ideal geometry.

1. Characterization, Structure and Crystallographic Data.

For Zn1/Zn1# in complex **1b**

```
-------------------------------------------------------------------------------
S H A P E   v2.1         Continuous Shape Measures calculation
(c) 2013 Electronic Structure Group, Universitat de Barcelona
                   Contact:  llunell@ub.edu
-------------------------------------------------------------------------------

ZnL2 structures

PP-5         1    D5h    Pentagon
vOC-5        2    C4v    Vacant octahedron
TBPY-5       3    D3h    Trigonal bipyramid
SPY-5        4    C4v    Spherical square pyramid
JTBPY-5      5    D3h    Johnson trigonal bipyramid J12

For Zn1/Zn1#
Structure [ML5]      PP-5        vOC-5       TBPY-5        SPY-5      JTBPY-5
Complex (1b),       35.869,      5.680,      1.231,        2.722,      4.282
```

[a]CShM values between 0.1 and 3 usually correspond to a not negligible but still small distortion from ideal geometry.

For Zn/Zn1# in complex **1c**

```
-------------------------------------------------------------------------------
S H A P E   v2.1         Continuous Shape Measures calculation
(c) 2013 Electronic Structure Group, Universitat de Barcelona
                   Contact:  llunell@ub.edu
-------------------------------------------------------------------------------

ZnL2 structures

PP-5         1    D5h    Pentagon
vOC-5        2    C4v    Vacant octahedron
TBPY-5       3    D3h    Trigonal bipyramid
SPY-5        4    C4v    Spherical square pyramid
JTBPY-5      5    D3h    Johnson trigonal bipyramid J12

For Zn1/Zn1#
Structure [ML5]      PP-5        vOC-5       TBPY-5        SPY-5      JTBPY-5
Complex (1c),       36.381,      6.717,      1.646,        3.354,      5.157
```

[a]CShM values between 0.1 and 3 usually correspond to a not negligible but still small distortion from ideal geometry.

1. Characterization, Structure and Crystallographic Data.

For Cd2/Cd2# in complex **2**

```
-------------------------------------------------------------------------------
S H A P E   v2.1         Continuous Shape Measures calculation
(c) 2013 Electronic Structure Group, Universitat de Barcelona
                   Contact:  llunell@ub.edu
-------------------------------------------------------------------------------

Cd3L2 structures

HP-7            1 D7h   Heptagon
HPY-7           2 C6v   Hexagonal pyramid
PBPY-7          3 D5h   Pentagonal bipyramid
COC-7           4 C3v   Capped octahedron
CTPR-7          5 C2v   Capped trigonal prism
JPBPY-7         6 D5h   Johnson pentagonal bipyramid J13
JETPY-7         7 C3v   Johnson elongated triangular pyramid J7

For Cd2/Cd2#
Structure [ML7]  HP-7        HPY-7       PBPY-7     COC-7       CTPR-7     JPBPY-7      JETPY-7
Complex (2),    33.802,    20.797,     8.069,     6.990,     5.786,     10.081,      14.081


Cd3L3 structures

HP-6            1 D6h   Hexagon
PPY-6           2 C5v   Pentagonal pyramid
OC-6            3 Oh    Octahedron
TPR-6           4 D3h   Trigonal prism
JPPY-6          5 C5v   Johnson pentagonal pyramid J2

For Cd2/Cd2#
Structure [ML6]  HP-6        PPY-6         OC-6        TPR-6       JPPY-6
Complex (2),    23.649,      5.572,       15.070,      6.255,      8.780
```

[a]CShM values between 0.1 and 3 usually correspond to a not negligible but still small distortion from ideal geometry.

1. Characterization, Structure and Crystallographic Data.

For Cd1 in complex **2**

```
-------------------------------------------------------------------------------
S H A P E   v2.1         Continuous Shape Measures calculation
(c) 2013 Electronic Structure Group, Universitat de Barcelona
                   Contact:  llunell@ub.edu
-------------------------------------------------------------------------------

Cd3L2 structures

OP-8          1      D8h       Octagon
HPY-8         2      C7v       Heptagonal pyramid
HBPY-8        3      D6h       Hexagonal bipyramid
CU-8          4      Oh        Cube
SAPR-8        5      D4d       Square  antiprism
TDD-8         6      D2d       Triangular dodecahedron
JGBF-8        7      D2d       Johnson gyrobifastigium J26
JETBPY-8      8      D3h       Johnson elongated triangular bipyramid J14
JBTPR-8       9      C2v       Biaugmented trigonal prism J50
BTPR-8       10      C2v       Biaugmented trigonal prism
JSD-8        11      D2d       Snub diphenoid J84
TT-8         12      Td        Triakis tetrahedron
ETBPY-8      13      D3h       Elongated trigonal bipyramid
For Cd1
Structure [ML8]   OP-8    HPY-8    HBPY-8   CU-8   SAPR-8  TDD-8    JGBF-8  JETBPY-8   JBTPR-8
Complex (2),     30.572, 23.480,  15.039,  9.889,  3.565,  2.641,   14.979,  24.634,    4.356,

                  BTPR-8  JSD-8    TT-8    ETBPY-8
                  4.253,  4.348,  10.078,  18.859
```

[a]CShM values between 0.1 and 3 usually correspond to a not negligible but still small distortion from ideal geometry.

Table S5. Parameters used for determining nitrate coordination mode and appropriate values for the coordinated nitrate group in complexes **1(a)** and **2**.

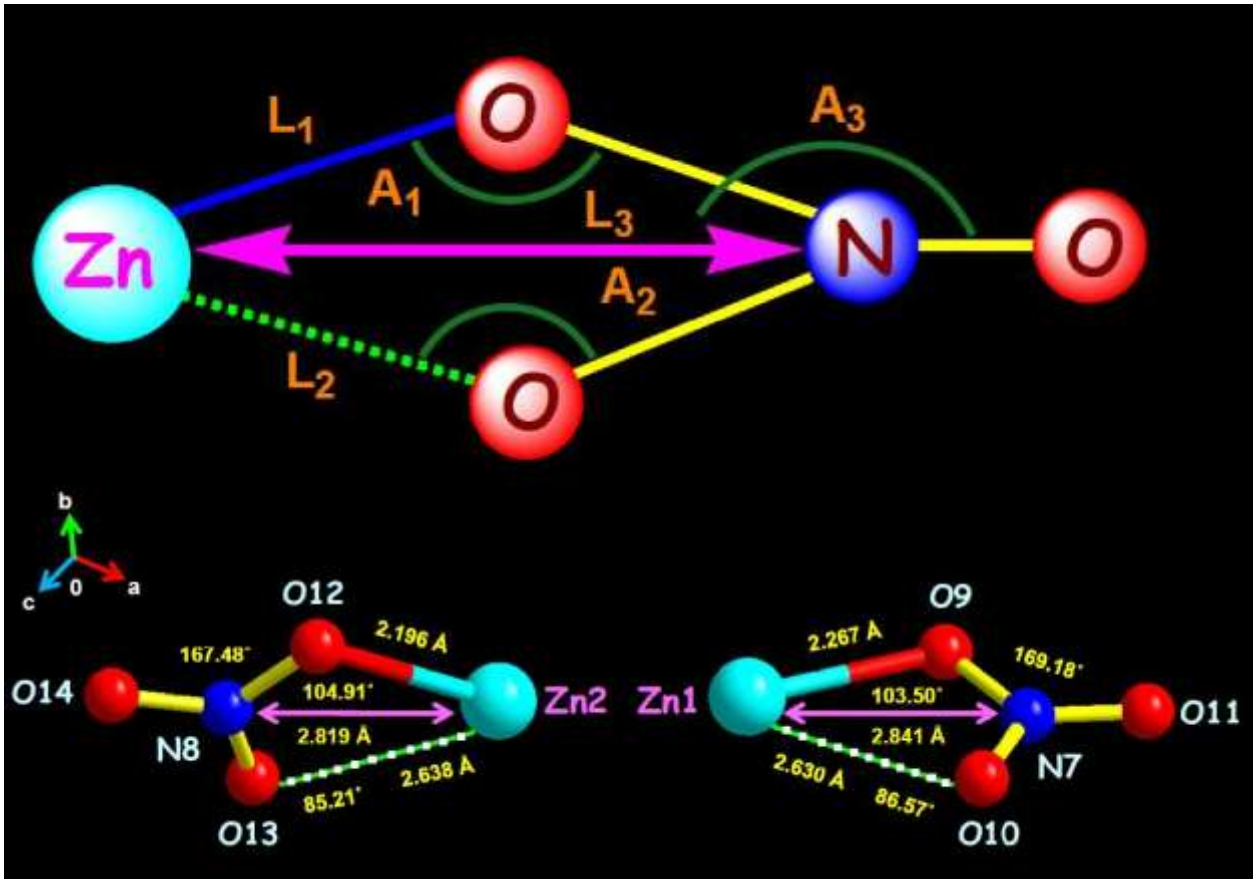

	Monodentate	Anisobidentate	Bidentate	Complex **1a**	
				Zn2	Zn1
L_2–L_1 (Å)	>0.6	0.3–0.6	<0.3	0.442	0.363
A_1–A_2(º)	>28	14–28	<14	19.7	16.93
L_3–L_2 (Å)	<0.1	0.1–0.2	>0.2	0.181	0.211
A_3 (º)	<162	162–168	>168	167.48	169.18

1. Characterization, Structure and Crystallographic Data.

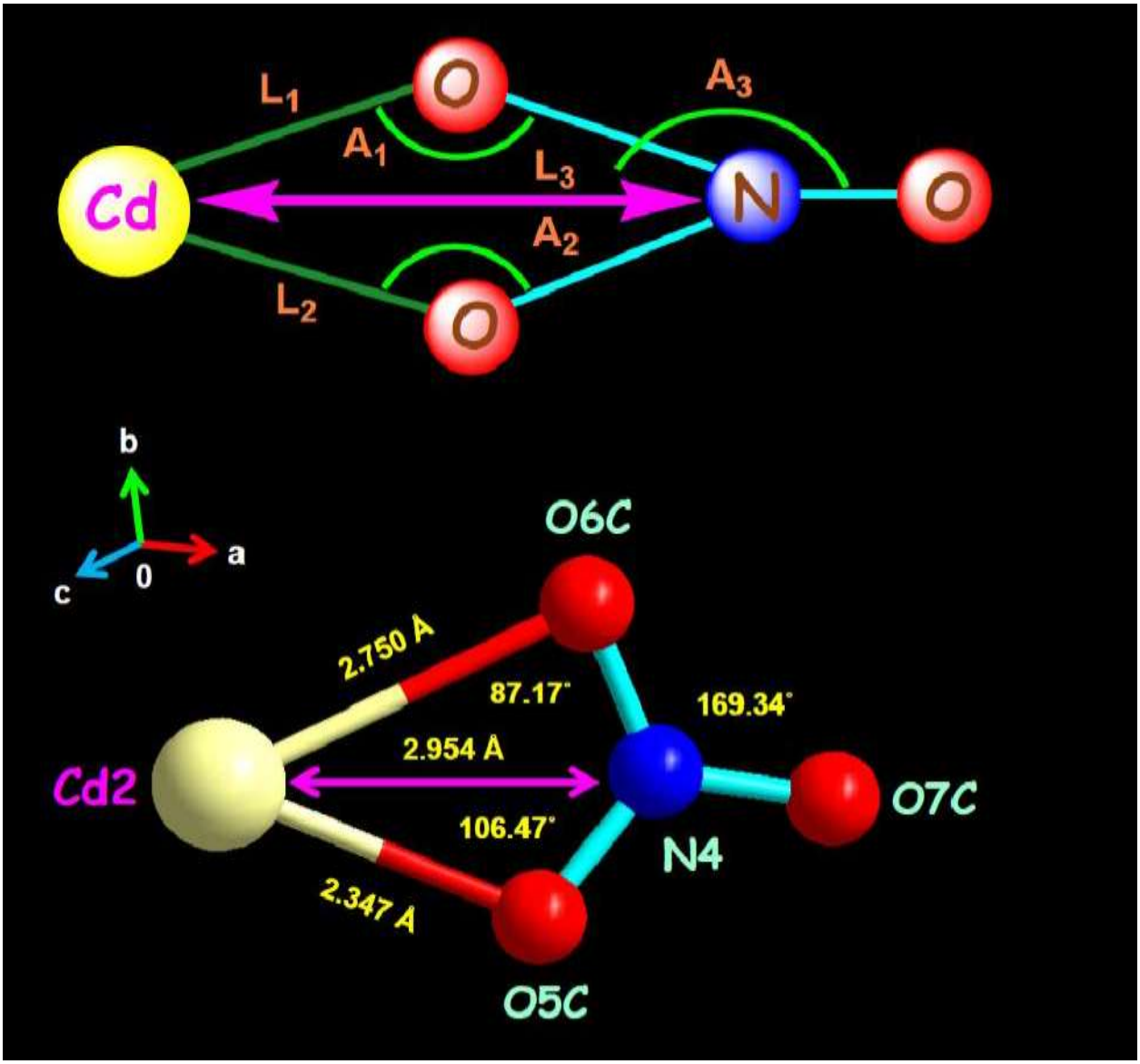

	Monodentate	Anisobidentate	Bidentate	Complex **2**
L_2–L_1 (Å)	>0.6	0.3–0.6	<0.3	0.403
A_1–A_2(º)	>28	14–28	<14	19.3
L_3–L_2 (Å)	<0.1	0.1–0.2	>0.2	0.607
A_3 (º)	<162	162–168	>168	169.34

Table S6. Hydrogen bonds (distances, Å, angles ^{o}) in the complexes **1(a-c)−2**.

Complex 1a			
N-H···O	H···O	N···O	N-H···O
N5-H5B···O2	1.89	2.730(4)	157
N5-H5B···O4	2.51	3.116(4)	126
N5-H5A···O1	1.94	2.764(4)	154
N5-H5A···O3	2.51	3.160(4)	131
N2-H2A···O5	1.91	2.744(5)	156
N2-H2A···O7	2.49	3.149(5)	131
N2-H2B···O6	1.88	2.723(4)	158
N2-H2B···O8	2.54	3.144(5)	126
O1S-H1S···O11	1.94	2.752(8)	170

Complex 1b			
N-H···O	H···O	N···O	N-H···O
N2-H2A···O1[a]	1.83	2.692(4)	159
N2-H2A···O2[a]	2.45	3.023(4)	122
[a]Symmetry element 1-x, 1/2-y, z			

Complex 1c			
N-H···O	H···O	N···O	N-H···O
N2-H2A···O1[a]	1.82	2.687(4)	159
N2-H2A···O2[a]	2.45	3.014(4)	122
[a]Symmetry element 1-x, 1/2-y, z			

Complex 2				
D--H···A	d(D—H)	d(H···A)	d(D···A)	<(DHA)
C9-H9A···O5C	0.97	2.55	3.171(6)	122
C12-H12···O6C	0.93	2.42	3.305(6)	160

1. Characterization, Structure and Crystallographic Data.

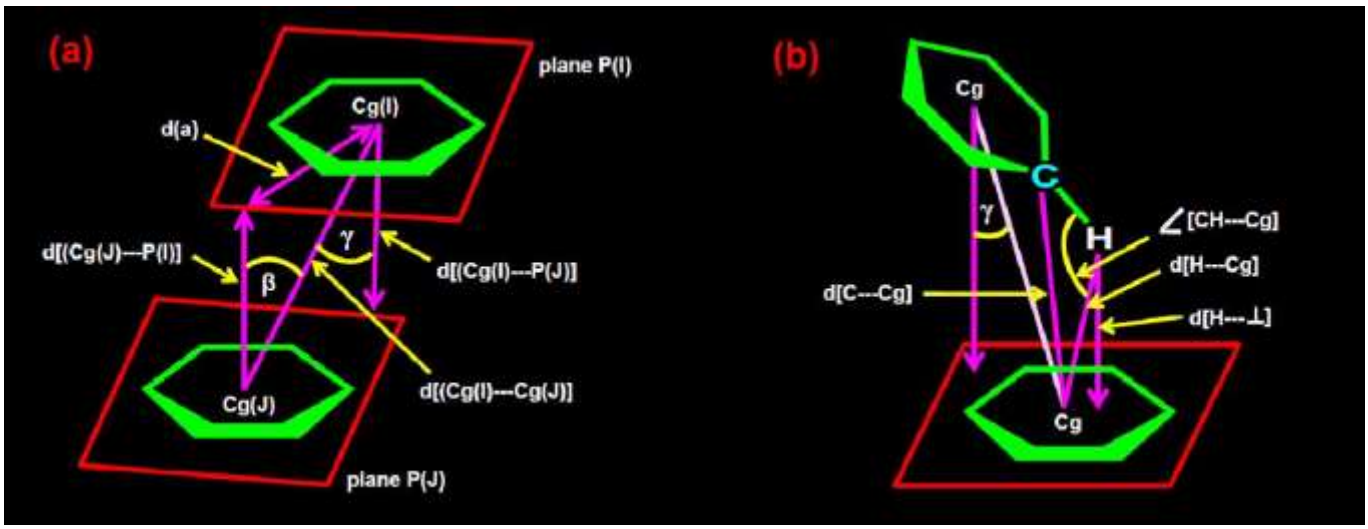

Scheme S1. Graphical presentation of the parameters used in Table S7. for the description of (a) π···π stacking and (b) CH···π interactions in complexes **1(a-c)−2**.

Table S7. Distances (d/Å) and angles (°) for the π-contacts in the crystal structures of complexes **1(a-c)−2**.

Complex, **π-π** interactions ring(I)···ring(J)	d[Cg(I)···Cg(J)][b]	α[c]	β[d]	γ[e]	d[Cg(I)···P(J)][f]	d[Cg(J)···P(I)][g]	d[a][h]
Complex1**a** Cg(7)···Cg(10)	3.619(3)	9.4(2)	14.9	9.6	3.5690(19)	3.4981(17)	0.93 0.60
Complex1**a** Cg(8)···Cg(9)	3.508(3)	8.9(2)	9.0	7.0	3.4812(19)	3.4647(19)	0.55 0.43
Complex1**b** Cg(3)···Cg(3)	3.778(3)	7.5(2)	21.6	21.6	3.5137(18)	3.5136(18)	1.39
Complex1**c** Cg(3)···Cg(3)	3.829(3)	9.7(2)	21.1	21.1	3.5726(18)	3.5727(18)	1.38
Complex**2** Cg(1)···Cg(1)	3.697(3)	9.1(2)	21.0	21.0	3.4504(19)	3.4506(19)	1.33
Complex, **CH-π** interactions ligand-C-H···ring	d[H···Cg][i]	d[H···⊥][j]	γ[e]	∠[CH···Cg][k]	d[C···Cg][l]		
Complex1**a** [C11–H11A ···Cg(9)]	2.75	2.68	12.83	156	3.658(5)		

Complex1**b** [C10–H10A ···Cg(3)]	2.89	2.72	20.01	125	3.533(5)		
Complex1**c** [C10–H10A ···Cg(3)]	2.91	2.78	17.60	128	3.579(5)		
Complex**2** [C19–H19C ···Cg(1)]	2.73	2.71	7.09	149	3.588(5)		

[a]For a graphical depiction of distances and angles in the assessment of the π-contacts, see Scheme S1. [b]Centroid to centroid distance. [c]Dihedral angle between the ring planes. [d]Angle between the centroid vector Cg(I)···Cg(J) and the normal to the plane I. [e]Angle between the centroid vector Cg(I)···Cg(J) and the normal to the plane J. [f] Perpendicular distance of Cg(I) from ring plane J. [g]Perpendicular distance of Cg(J) from ring plane I. [h]Vertical displacement between ring centroids. [i]H-centroid distance. [j]Perpendicular distance of H from ring plane. [k]C-H-centroid angle. [l]C-centroid distance.

Complex1**a**

Cg(7) = C1 --> C2 --> C3 --> C4 --> C5 --> C6 ring

Cg(10) = C33 --> C34 --> C35 --> C36 --> C37 --> C38 ring

Cg(8) = C13 --> C14 --> C15 --> C16 --> C17 --> C18 ring

Cg(9) = C21 --> C22 --> C23 --> C24 --> C25 --> C26 ring

Complex1**b** and Complex1**c**

Cg(3) = C(1) --> C(2) --> C(3) --> C(4) --> C(5) --> C(6) ring

Complex**2**

Cg(1) = C(1) --> C(2) --> C(3) --> C(4) --> C(5) --> C(6) ring

1. Characterization, Structure and Crystallographic Data.

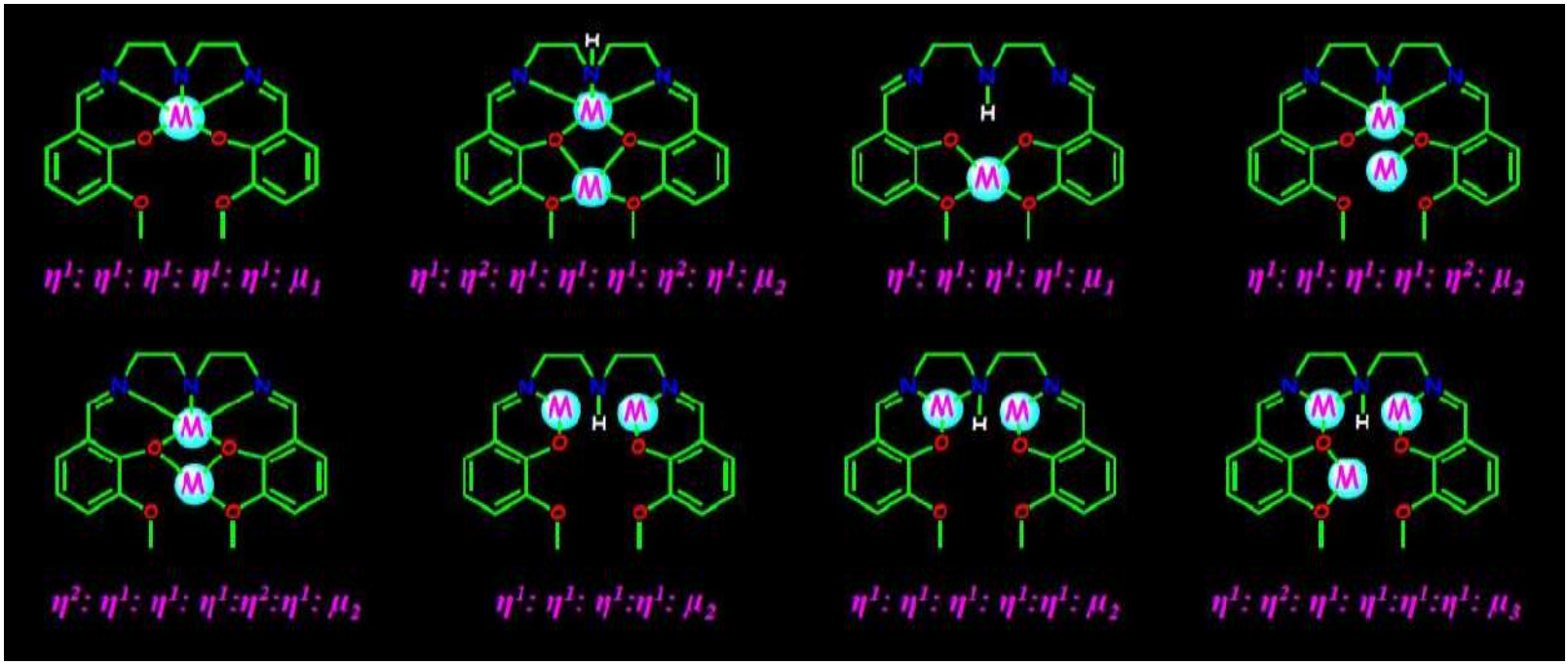

Scheme S2. Different Coordination modes exhibited by the ligand **(H_2Vd)** in the literature.

2. Photophysical Characterization.

UV–Vis spectra of **H_2Vd** upon titration with Zn^{2+} ion.

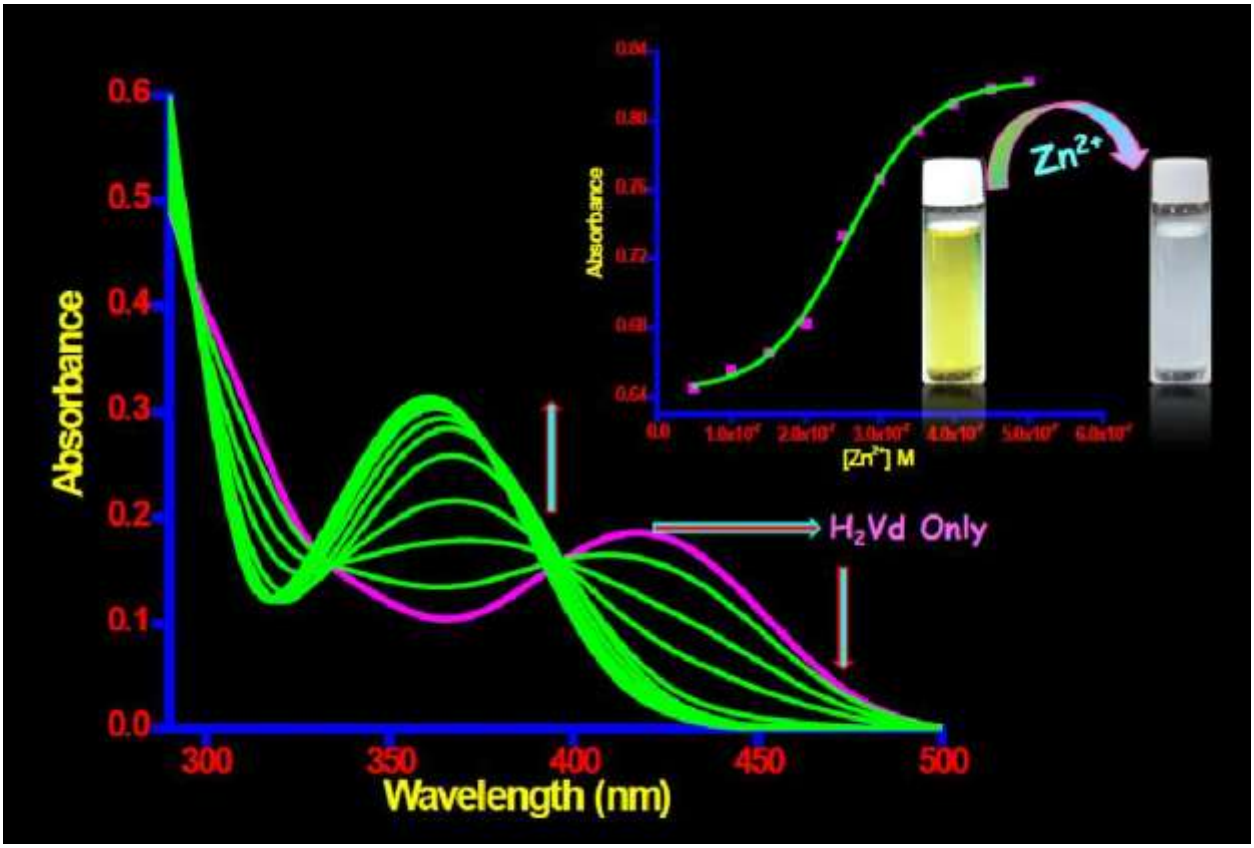

Figure S12. UV-vis spectra of **H_2Vd** (5×10^{-7}M) in HEPES buffer (pH = 7.4) solution in the presence of various concentrations of Zn^{2+} (0, 0.5, 1, 1.5, 2, 2.5, 3, 4 and 5) $\times10^{-7}$ M. **Inset:** Absorbance of **H_2Vd** at 360 nm as a function of [Zn^{2+}] and visual color change (yellow to colorless) observed with addition of Zn^{2+} ion to **H_2Vd** solution.

2. Photophysical Characterization.

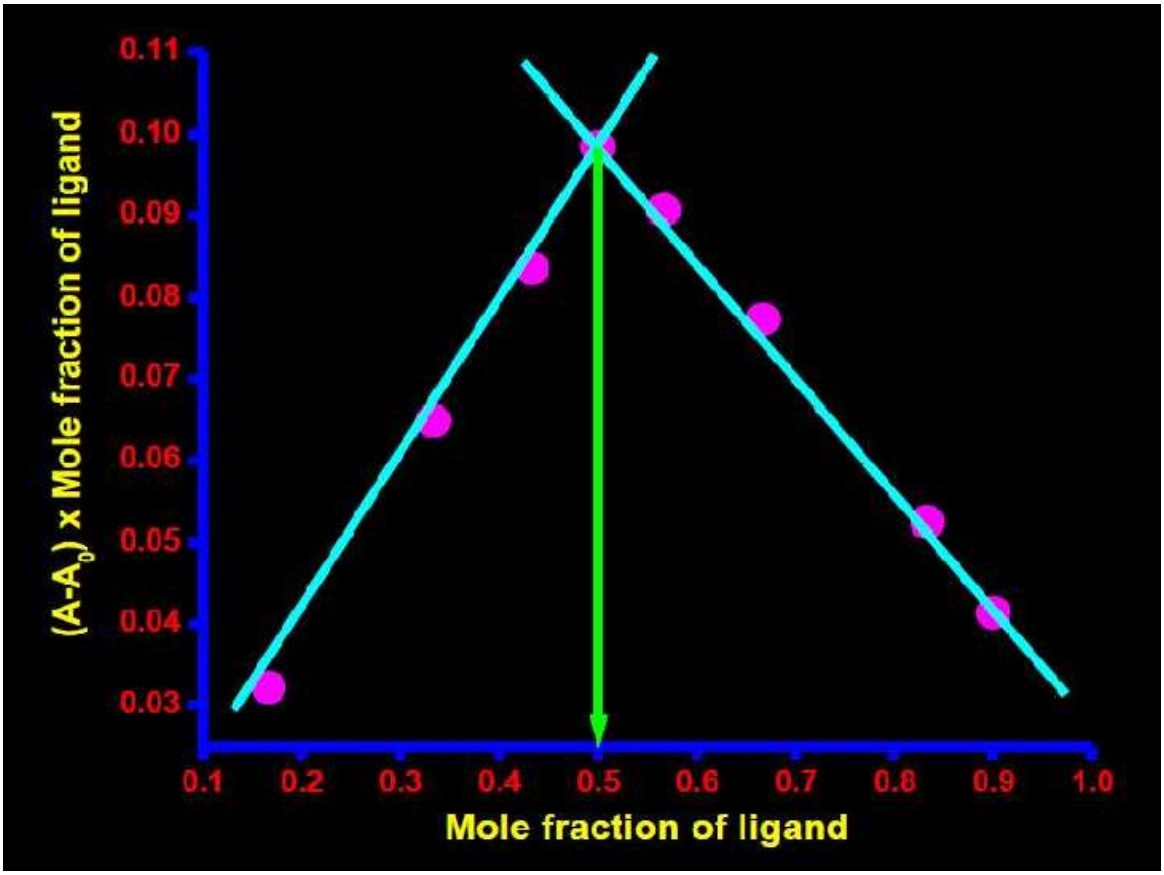

Figure S13. Job′s plot for the identification of **H_2Vd-**Zn^{2+} (1:1) complex stoichiometry using absorbance values at 360 nm.

2. Photophysical Characterization.

The binding constant (*K*) determined by the Benesi−Hildebrand expression was found to be $34.362 \times 10^4\ M^{-1}$.

$$\frac{1}{(A - A_0)} = \frac{1}{\{K(A_{max} - A_0)[C]\}} + \frac{1}{(A_{max} - A_0)}$$

Where A_0 is the absorbance of free ligand, *A* is the observed absorbance at that particular wavelength in the presence of a certain concentration of the metal ion *[C]*, A_{max} is the maximum absorbance value of the complex formed. *K* is the association constant (M^{-1}) and was determined from the slope of the linear plot and *[C]* is the concentration of the Zn^{2+} ion added during titration studies. The goodness of the linear fit of the B–H plot of $1/(A - A_0)$ *vs.* $1/[Zn^{2+}]$ for 1:1 complex formation confirms the binding stoichiometry between **H_2Vd** and Zn^{2+}.

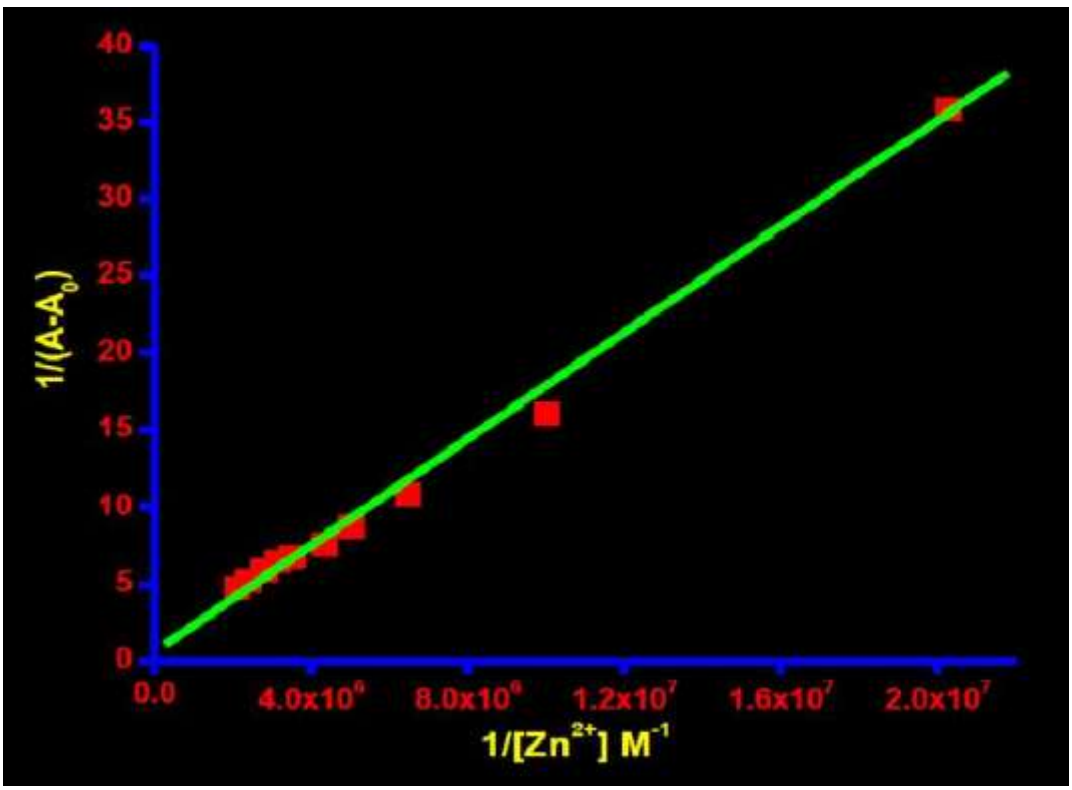

Figure S14. Benesi-Hildebrand plot of absorbance titration curve of **H_2Vd** and $[Zn^{2+}]$.

2. Photophysical Characterization.

According to the linear Benesi–Hildebrand expression, the measured fluorescence intensity $(F - F_0)/(F_x - F_0)$ at 467 nm varied as a function of $1/[Zn^{2+}]$ in a linear relationship, which indicates the formation of 1 : 1 stoichiometry between Zn^{2+} and **H_2Vd** in the complex.

$$\frac{1}{F_X - F_O} = \frac{1}{F_{max} - F_O} + \frac{1}{K[C]}\left(\frac{1}{F_{max} - F_O}\right)$$

where F_0, F_x and F_{max} are the emission intensities of organic moiety considered in the absence of Zn^{2+} ions, at an intermediate Zn^{2+} concentration and at a concentration of complete interaction, respectively, K is the binding constant and $[C]$ is the concentration of Zn^{2+} ions.

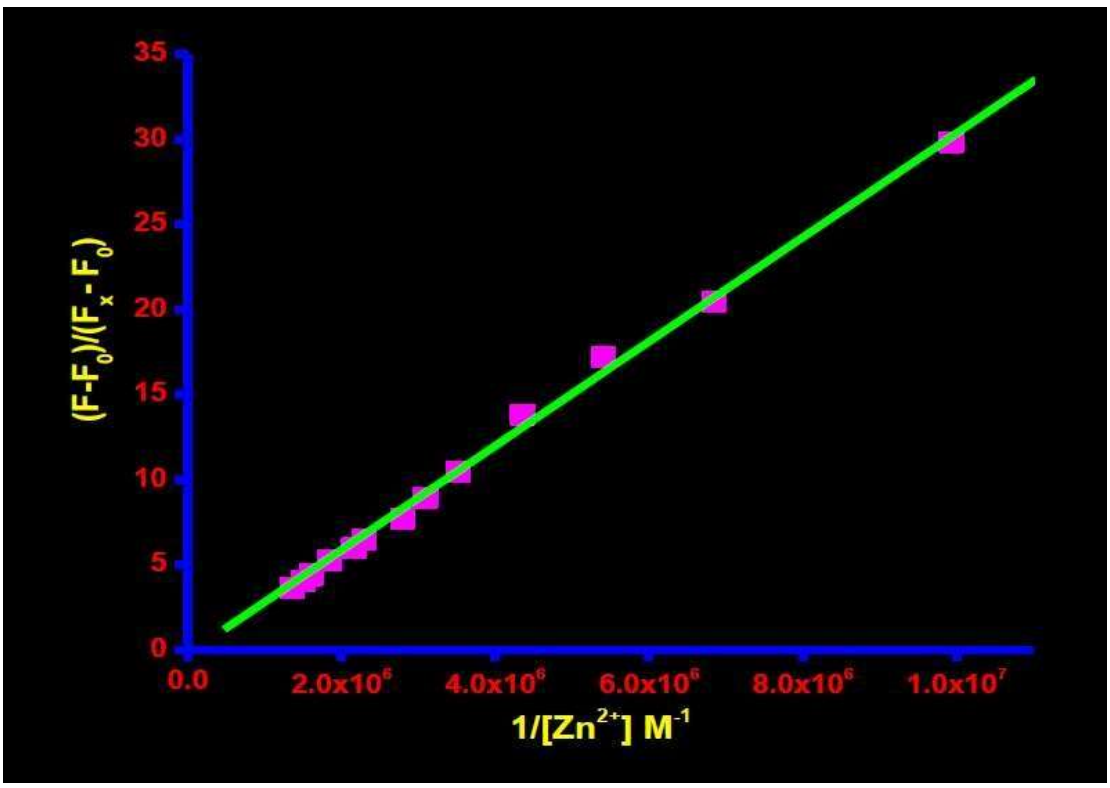

Figure S15. Benesi-Hildebrand plot $[F-F_0/F_x-F_0]$ vs. $1/[Zn^{2+}]$ for complexation between **H_2Vd** and Zn^{2+} derived from emission titration curve.

Detection limit calculation in emission spectroscopy.

The limit of detection (LOD) of **H_2Vd**–Zn^{2+} was measured on the basis of fluorescence titration measurement. The detection limit was calculated using the following equation:

$$DL = K \times \frac{o}{S}$$

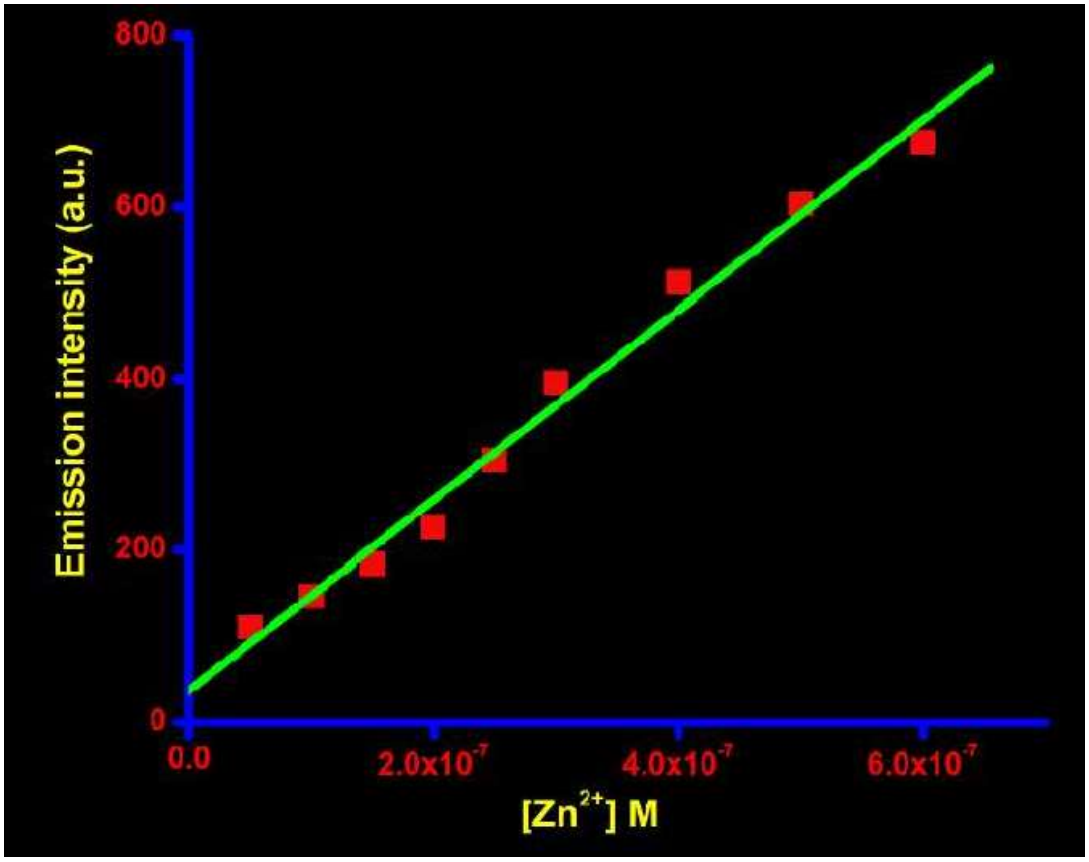

Figure S16. The limit of detection (LOD) of **H_2Vd** for Zn^{2+} fluorescence responses (λ_{em} = 467 nm) as a function of [Zn^{2+}].

2. Photophysical Characterization.

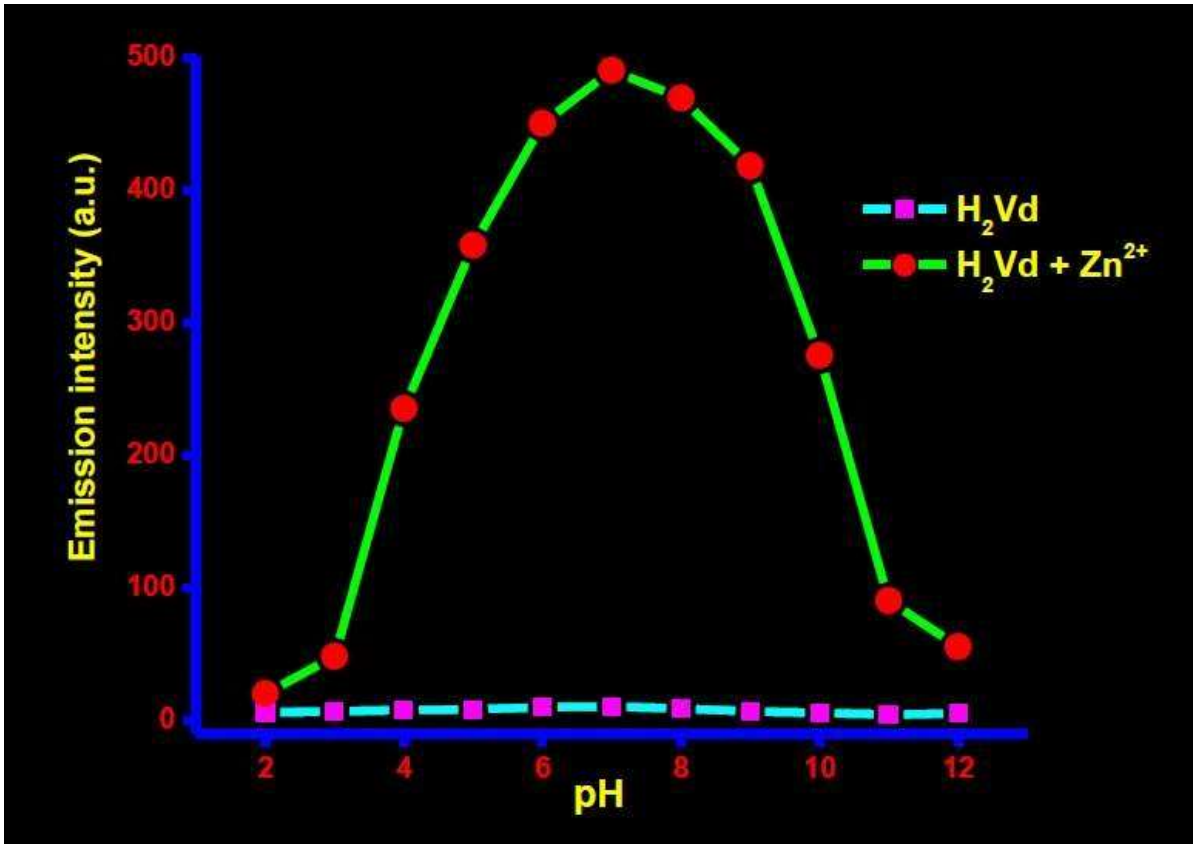

Figure S17. Emission intensity of probe **H_2Vd** (5×10^{-7} M) in the absence and in presence of Zn^{2+} as a function of pH values in aqueous solution at 467 nm.

2. Photophysical Characterization.

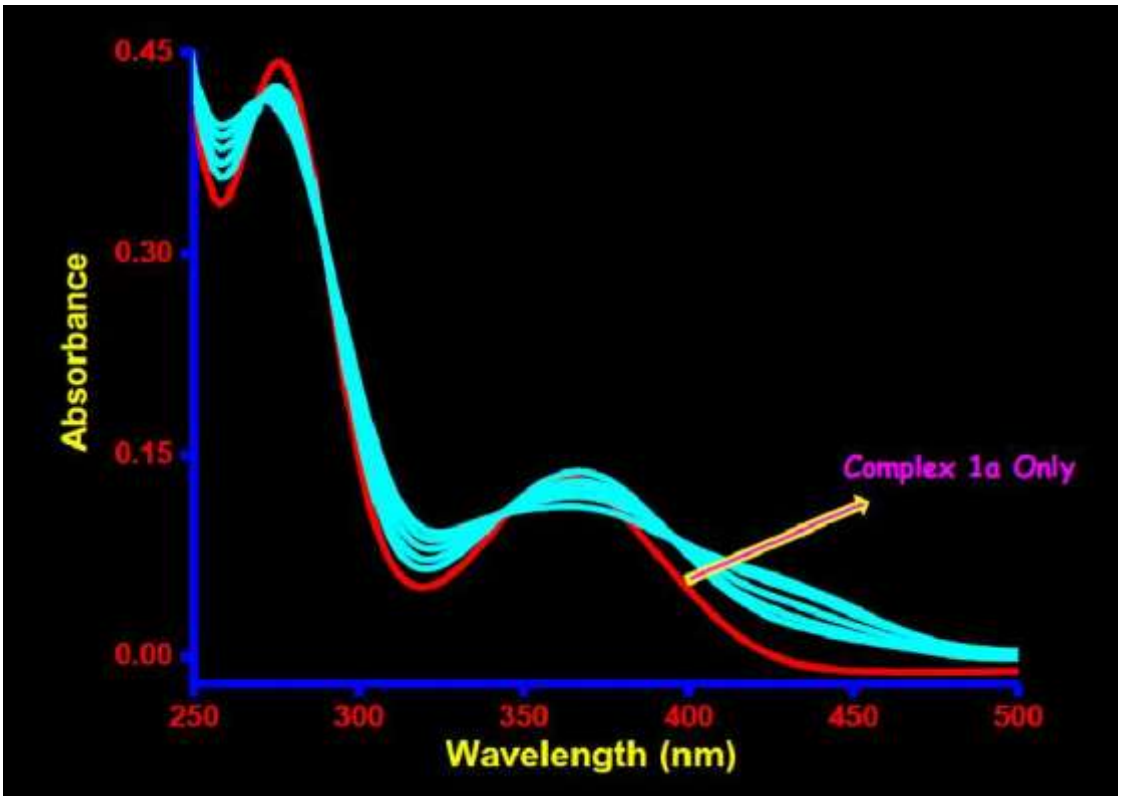

Figure S18. UV-vis spectra of complex **1a** (5×10^{-7} M) in HEPES buffer (pH = 7.4) solution in the presence of various concentration of PPi (0, 1, 2, 3, 4 and 5) $\times10^{-7}$ M.

2. Photophysical Characterization.

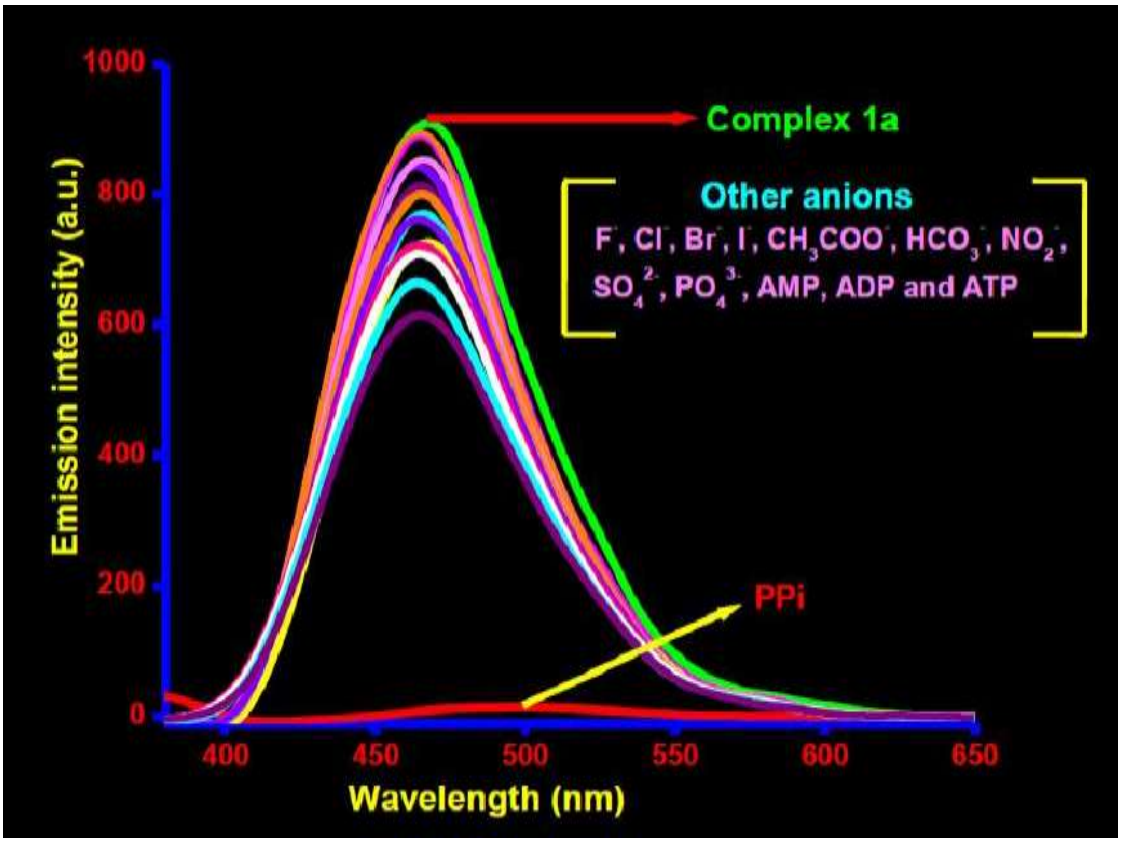

Figure S19. Fluorescence spectra of complex **1a** (5×10^{-7} M) upon the addition of different anions (10×10^{-7} M) in HEPES buffer (pH = 7.4) solution.

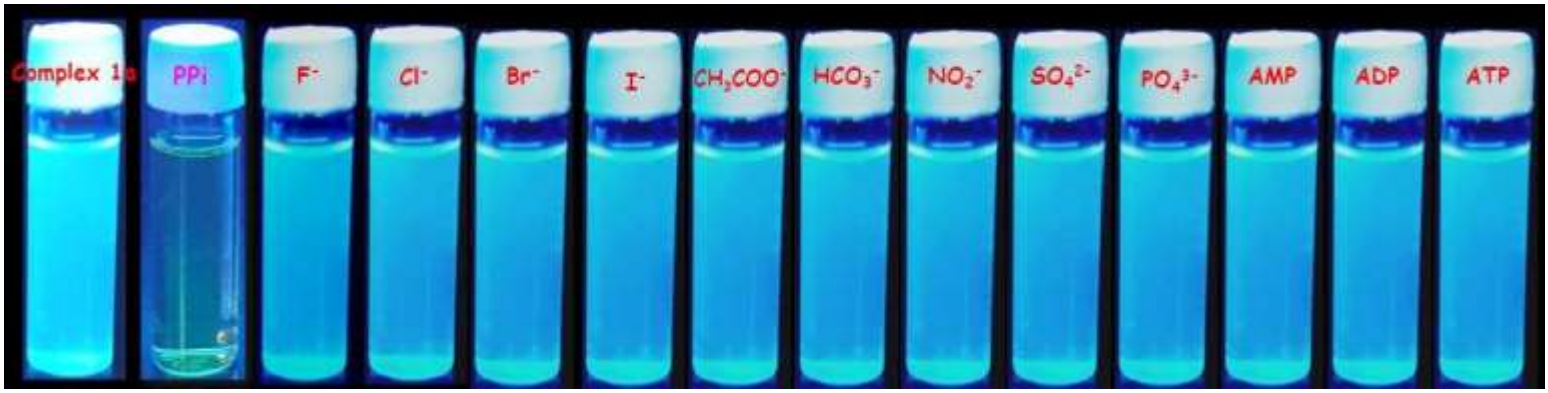

Figure S20. Visual color change observed with the addition of various anions to complex **1a** as seen under UV light (λ = 365 nm).

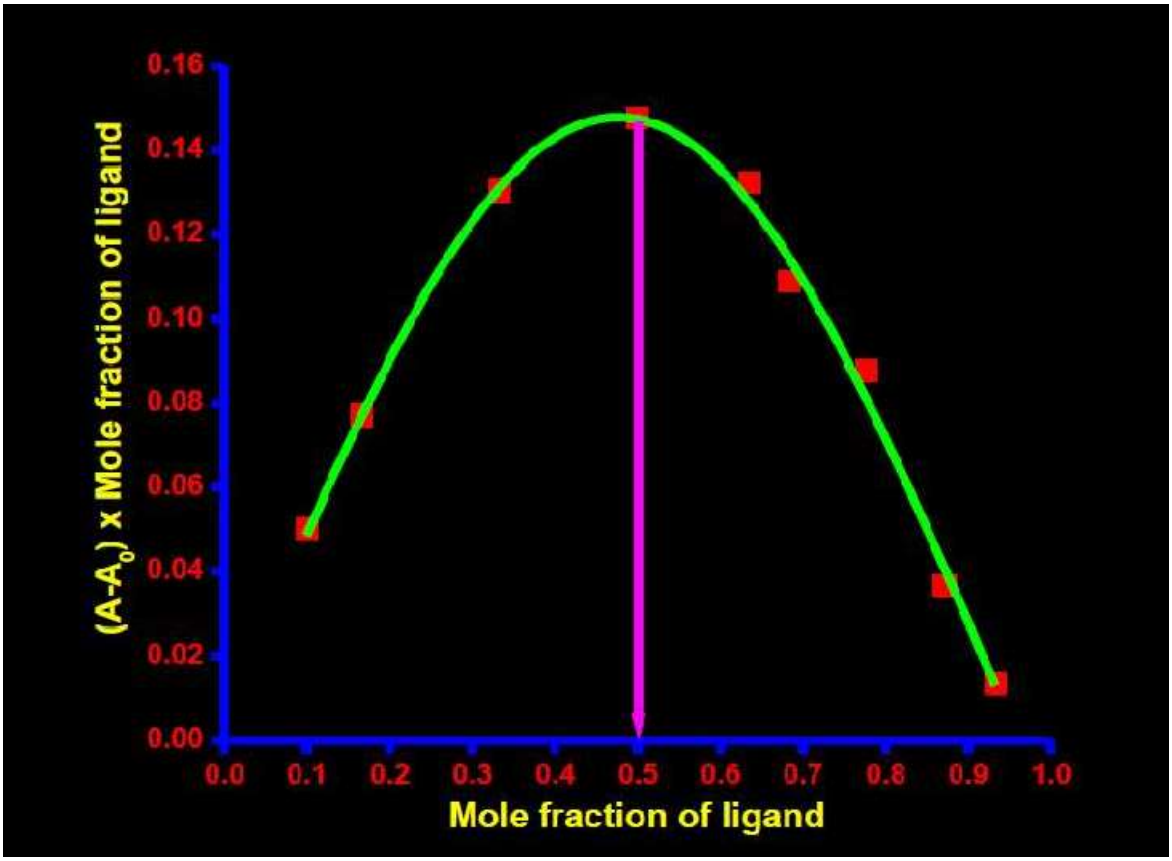

Figure S21. Job′s plot for the identification of complex **1a-**PPi (1:1) complex stoichiometry using absorbance values at 368 nm.

2. Photophysical Characterization.

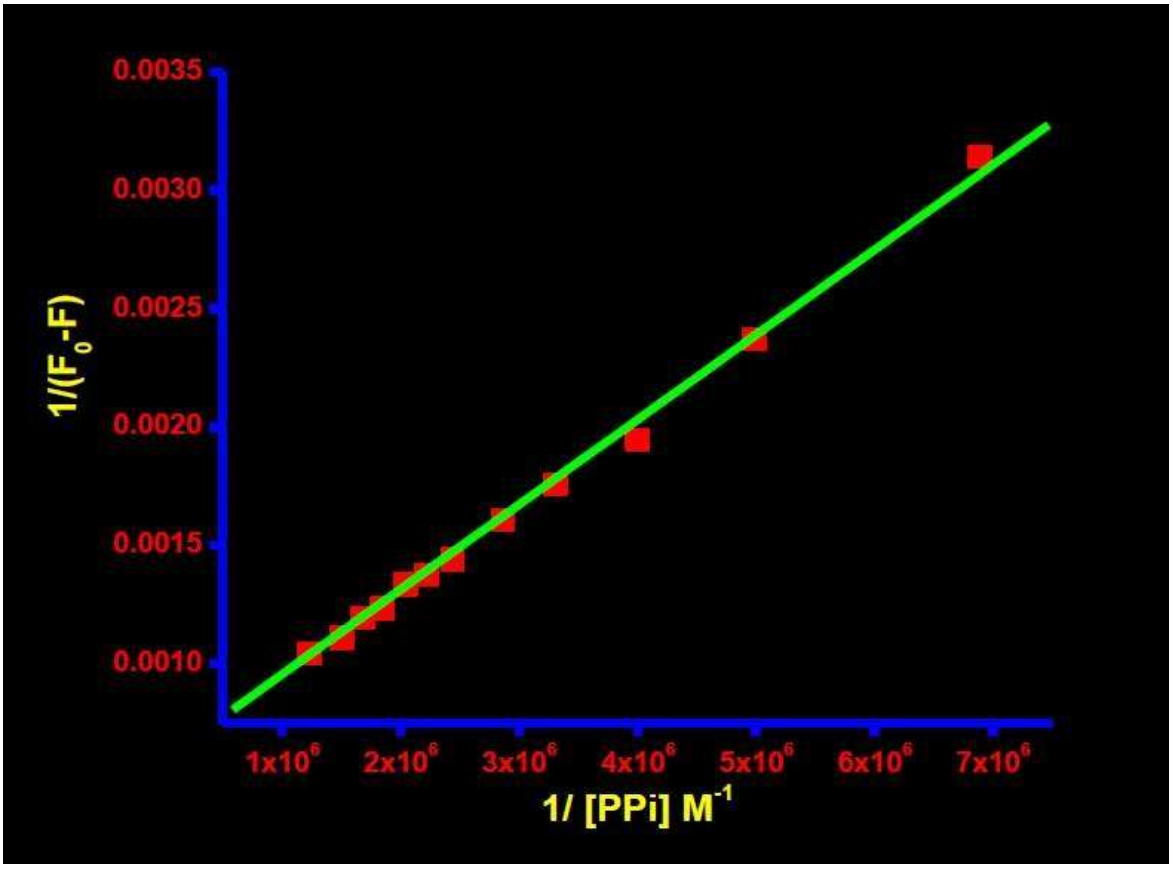

Figure S22. Benesi−Hildebrand plot *1 / (F_0 − F)* vs. *1/ [PPi]* for complexation between complex **1a** and PPi derived from emission titration curve.

2. Photophysical Characterization.

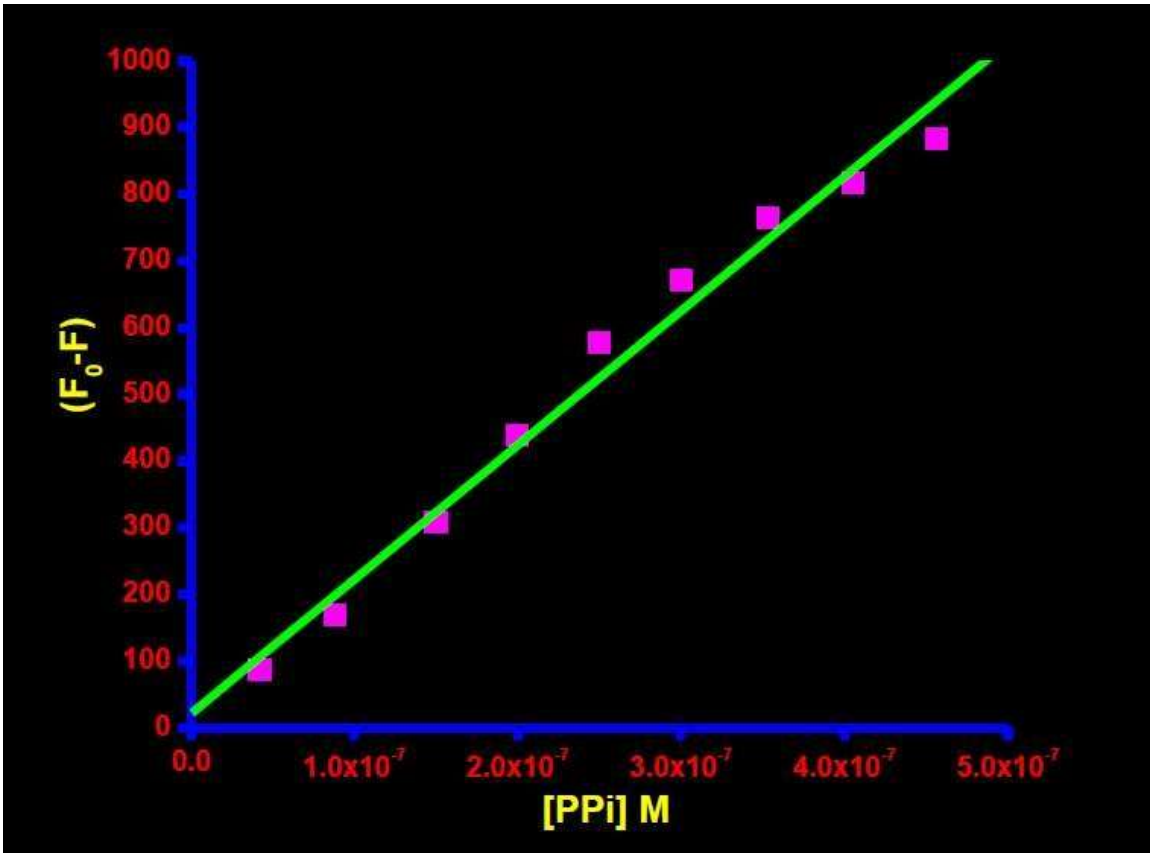

Figure S23. The limit of detection (LOD) of complex **1a** for PPi fluorescence responses (λ_{em}= 478 nm) as a function of PPi concentration.

2. Photophysical Characterization.

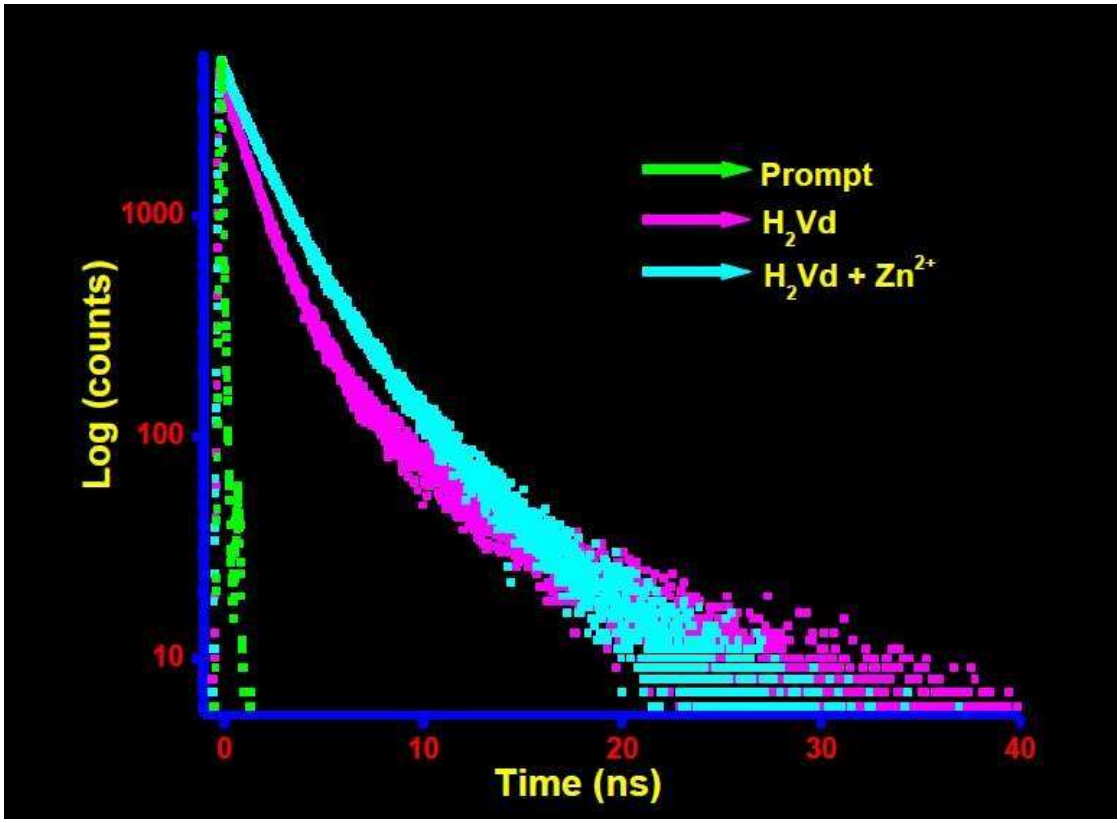

Figure S24. Time–resolved fluorescence decay of **H_2Vd** in the absence and presence of added Zn^{2+} solution at 375 nm.

2. Photophysical Characterization.

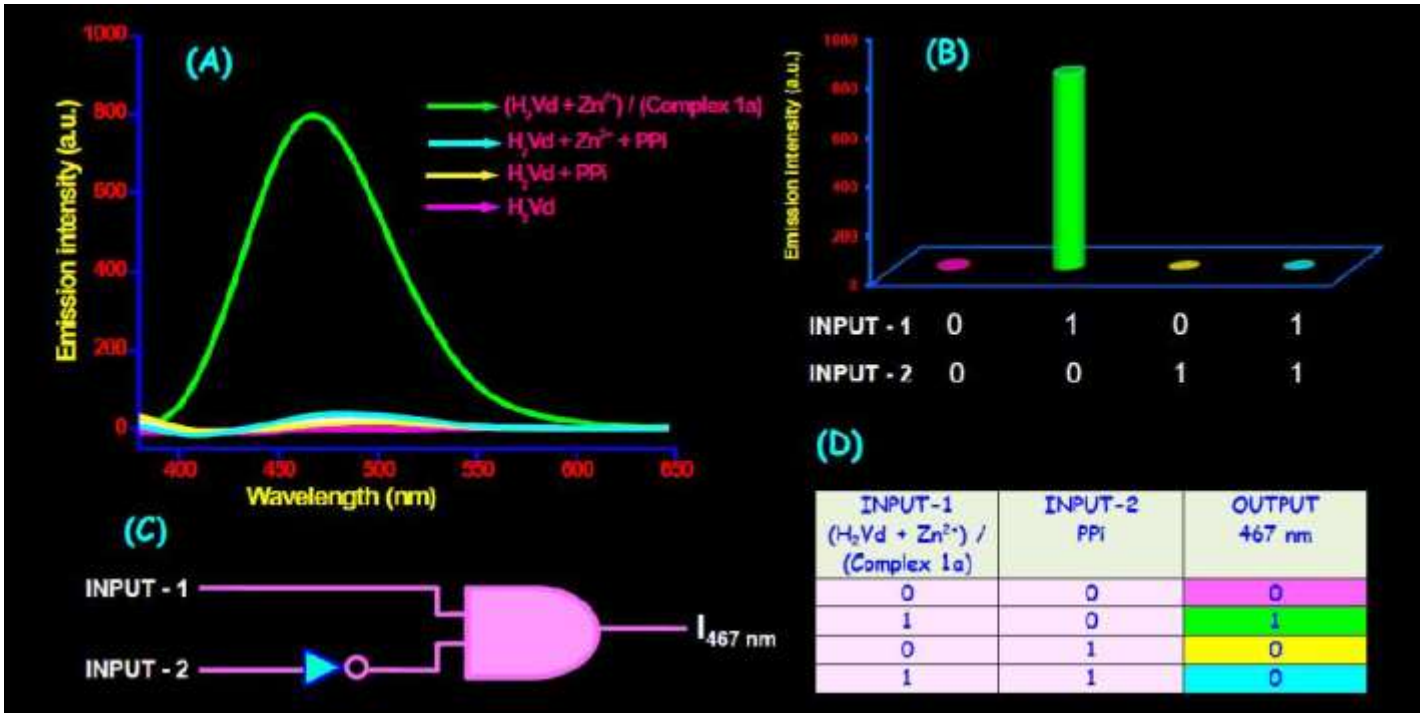

Figure S25. (A) Output signals (at 467 nm) of the logic gate in presence of different inputs. (B) The current signals of this logic gate in the presence of different inputs. (C) General representation of the symbol of an INHIBIT gate. (D) Corresponding truth table for two-input INHIBIT logic gate.

Table S8. Fluorescence lifetime measurement of chemosensor **H_2Vd** and the presence of Zn^{2+} in aqueous solution.

	φ_f	τ_{av}(ns)	K_r($\times10^9$) (S^{-1})	K_{nr}($\times10^9$) (S^{-1})	$\chi2$
H_2Vd	0.024	0.052	0.461	18.76	1.020
H_2Vd + Zn^{2+}	0.454	0.501	0.906	1.08	1.048

Table S9. Stability constant was compared with complexation properties of the other metal ions.

Different metal ions	Stability constant from absorption data (M^{-1})	Stability constant from fluorescence data (M^{-1})
Zn^{2+}	34.362×10^4	31.647×10^4
Li^{+}	1.287×10^3	1.355×10^3
Na^{+}	2.074×10^3	2.101×10^3
K^{+}	2.335×10^3	2.470×10^3
Ca^{2+}	2.402×10^3	2.343×10^3
Mg^{2+}	2.872×10^3	2.956×10^3
Mn^{2+}	1.919×10^3	1.861×10^3
Ba^{2+}	2.018×10^3	2.143×10^3
Cu^{2+}	1.598×10^3	1.712×10^3
Fe^{2+}	1.976×10^3	1.864×10^3
Cd^{2+}	1.459×10^4	1.501×10^4
Hg^{2+}	1.387×10^4	1.410×10^4
Ni^{2+}	2.507×10^3	2.204×10^3
Pb^{2+}	2.970×10^3	2.883×10^3
Sr^{2+}	2.737×10^3	2.698×10^3
Co^{2+}	1.142×10^3	1.215×10^3
Cr^{3+}	2.031×10^3	2.243×10^3
Al^{3+}	1.053×10^4	1.102×10^4

3. Cell study.

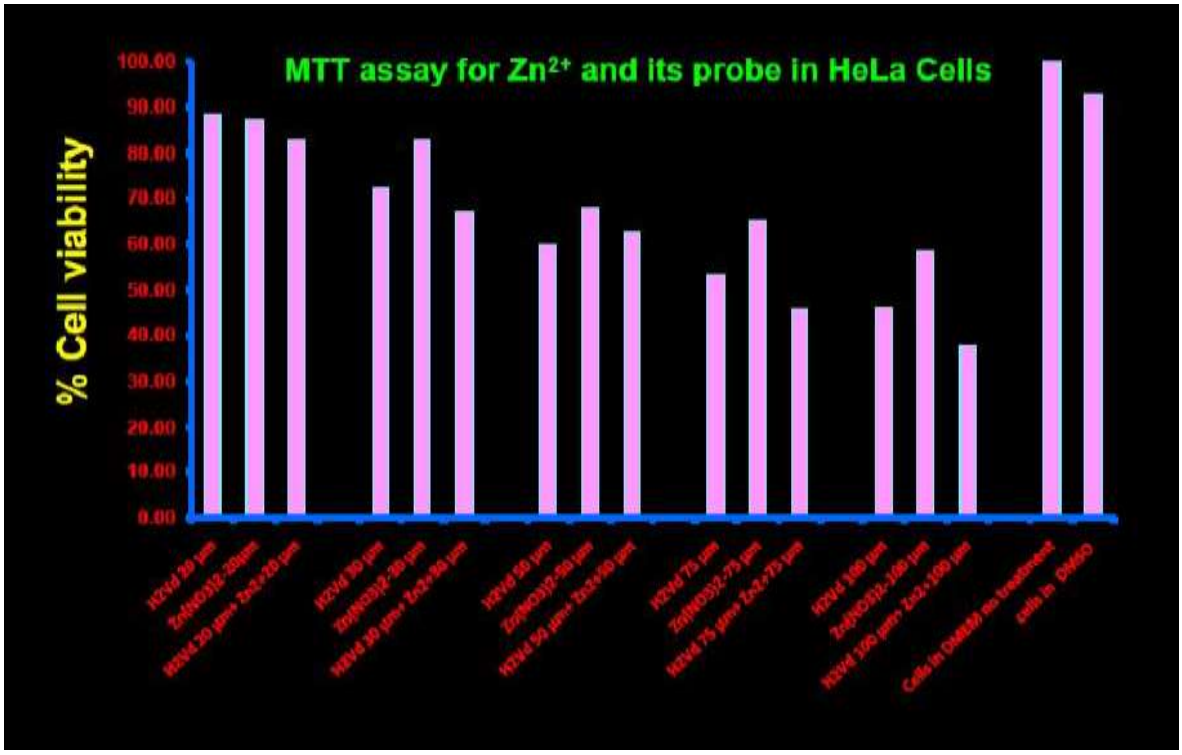

Figure S26. Percentage (%) cell viability of Hela cells treated with different concentrations of **H_2Vd** for 24 hours determined by MTT assay.